1-1-2006

Spectroscopic investigation of metal-substitution of cytochrome c

Deepthi Kandi

Eastern Illinois University

This research is a product of the graduate program in Chemistry at Eastern Illinois University. Find out more about the program.

THESIS REPRODUCTION CERTIFICATE

): Graduate Degree Candidates (who have written formal theses)

JBJECT: Permission to Reproduce Theses

ιe University Library is receiving a number of request from other institutions asking permission to reproduce dissertations for
:lusion in their library holdings. Although no copyright laws are involved, we feel that professional courtesy demands that
·rmission be obtained from the author before we allow these to be copied.

.EASE SIGN ONE OF THE FOLLOWING STATEMENTS:

·oth Library of Eastern Illinois University has my permission to lend my thesis to a reputable college or university for the purpose of
·pying it for inclusion in that institution's library or research holdings.

_____   11|17|06
·ιthor's Signature   Date

·ιspectfully request Booth Library of Eastern Illinois University **NOT** allow my thesis to be reproduced because:

_____

_____

_____

_____   _____
:hor's Signature   Date

·s form **must be submitted in duplicate.**

Spectroscopic Investigation of

Metal-Substitution in Cytochrome c

(TITLE)

BY

Deepthi Kandi

THESIS

SUBMITTED IN PARTIAL FULFILLMENT OF THE REQUIREMENTS
FOR THE DEGREE OF

Master of Science in Chemistry

IN THE GRADUATE SCHOOL, EASTERN ILLINOIS UNIVERSITY
CHARLESTON, ILLINOIS

2006
YEAR

I HEREBY RECOMMEND THAT THIS THESIS BE ACCEPTED AS FULFILLING
THIS PART OF THE GRADUATE DEGREE CITED ABOVE

11/16/2006

DATE

THESIS DIRECTOR

11/17/2006

DATE

DEPARTMENT/SCHOOL HEAD

Spectroscopic Investigation of Metal Substitution in Cytochrome *c*

Deepthi Kandi
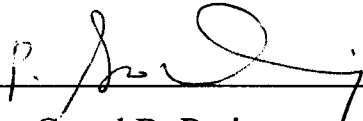
This thesis has been read and approved by each member of the following supervisory committee:

_____   11/16/2006
Dr. Jonathan P. Blitz   Date

_____   11/16/2006
Dr. Gopal R. Periyannan   Date

_____   11/16/2006
Dr. Scott M. Tremain   Date

_____   11/16/2006
Dr. Kraig A. Wheeler   Date

ACKNOWLEDGEMENTS

Table of Contents

iv

List of Figures

List of Tables

Table   **Page**

ABSTRACT

We study, by absorbance spectroscopy, the incorporation of various metal ions (Cu^{2+} and Zn^{2+}) into metal-free porphyrin cytochrome c (H_2cyt) as well as the various conformational forms of metal-substituted cytochromes. The H_2cyt and desired metal-substituted cytochromes have significantly different absorption spectra, providing a simple means of monitoring the incorporation of Cu^{2+} or Zn^{2+} into the empty porphyrin prosthetic group. The rates of metal-ion incorporation were studied under protein denaturing conditions using chemical denaturants, like urea and guanidine hydrochloride (GuHCl), and temperature that partially and completely unfold H_2cyt, facilitating the incorporation of a metal ion. Moreover, the structural stability of copper-substituted cytochrome c (Cucyt) was investigated using fluorescence spectroscopy.

In general, increasing concentrations of urea and GuHCl significantly affect the rate of metal-ion incorporation into H_2cyt and also lead to the appearance of various structural conformations of metal-substituted cytochromes that can be resolved via absorbance spectroscopy. At lower concentrations of denaturant, the rate of incorporation of a metal ion was slower due to less exposure of the buried porphyrin to solvent as cytochrome c is only partially unfolded. Moreover, metal-ion incorporation was incomplete, as some H_2cyt remained (confirmed by absorbance spectroscopy). However, at higher concentrations of denaturant, the rate of incorporation was rapid due to the highly solvent-accessible porphyrin in unfolded cytochrome c. No H_2cyt was spectroscopically observed after incorporation, indicating complete incorporation of the desired metal ion. Moreover, the rate constants for the decay of H_2cyt and the formation

of metal-substituted cytochrome *c* are similar, indicating a single step process without any intermediates.

Specifically, the rate constant for the incorporation of Zn^{2+} into H_2cyt initially increases as GuHCl concentration increases; however, above 2.0 M GuHCl, the rate constants remain unchanged. This indicates that at 2.0 M GuHCl, the porphyrin is already maximally accessible for Zn^{2+} incorporation. Overall, the rate of Cu^{2+} incorporation into H_2cyt is faster than Zn^{2+} incorporation.

Upon incorporation of Cu^{2+} into H_2cyt, various spectroscopic forms of Cucyt were observed. The shift in the heme Soret absorbance band was dependent on the concentration of GuHCl. At lower GuHCl concentrations (0.5 M & 1.0 M), two Soret absorbance bands at 403 nm and 422 nm were observed, indicating the presence of two different Cucyt structural conformations. At higher concentrations of GuHCl (2.5 M – 4.0 M), a single Soret absorbance band at 390 nm was observed, indicating a third Cucyt structural conformation. In drastic contrast to Cucyt, only one spectroscopic form of Zncyt has been observed under the same experimental conditions, with a Soret absorbance band at 423 nm. These different spectroscopic forms of Cucyt are most likely due to differences in the coordination environment of the Cu^{2+} ion upon changes in axial ligation.

In one experimental preparation of H_2cyt, incorporation of an unknown contaminating metal ion was observed prior to any addition of the desired metal ion salt solution to the cuvette solution. Prompted by this experimental observation, we wanted to determine the lowest concentration of GuHCl that still allowed contaminating metal ion incorporation. Metal-ion incorporation can be a sensitive probe of the protein's

tertiary structure and porphyrin accessibility. The goal was to incrementally lower the GuHCl concentration until no GuHCl-induced conformational changes in H_2cyt were observed. Even at very low GuHCl concentrations (0.1 M, 0.01 M, and 0.001 M), metal-ion incorporation was observed indicating GuHCl-induced conformation changes (i.e. partial protein unfolding and increased porphyrin accessibility). At 0.0001 M GuHCl, no GuHCl-induced conformational changes were observed.

To determine the structural stability of Cucyt, fluorescence spectroscopy was used to monitor the decrease in tryptophan fluorescence emission intensity as denaturant concentration increases. Urea-induced and GuHCl-induced equilibrium unfolding studies of Cucyt indicated a midpoint for the unfolding transition (C_m) in urea at 4.7±0.1 M and in GuHCl at 2.6±0.2 M. The extrapolated free energy for unfolding Cucyt in the absence of denaturant (ΔG_U) was 19.4±5.5 kJ/mol using GuHCl as a denaturant and 23.8±2.3 kJ/mol using urea as a denaturant.

CHAPTER 1.

INTRODUCTION

Goals. In our research, the overall goal is to better understand the role that metal ions play in the structural stability of heme proteins and to prepare novel metal-substituted derivatives of cytochrome c. The specific aims in this thesis are to prepare metal-substituted forms of cytochrome c, specifically zinc cytochrome c (Zncyt) and copper cytochrome c (Cucyt), measure the rates of Zn^{2+} and Cu^{2+} incorporation into metal-free porphyrin cytochrome c (H_2cyt), optimize the conditions for incorporation of each metal ion, and characterize the structural stability of these metal-substituted cytochromes.

Proteins. Proteins are the most abundant molecules in humans besides water. They constitute about 15% of the body weight with diverse roles in structure, communication, transport and catalysis. The characteristic properties of these proteins, as well as biological activity, depend on their ability to fold into a unique three-dimensional structure.[1]

Metals in Biological Systems. Metals are common natural constituents of proteins where the properties of metal ions are used to perform a variety of specific functions associated with biological processes.[2] Metal binding can be seen as a special case of protein:biological partner recognition.[3] Metal ions play major roles in transferring small molecules (O_2 for respiration), binding and activating substrates for catalysis (digestion and metabolism), providing structure (teeth and bone), and regulating

biological processes (muscle contraction).[2] Because of the widespread occurrence and biological importance in plants and animals, it has been an important field of study.[4]

Metalloproteins. Nearly one third of all proteins require metals as cofactors for their biological functions. Metalloproteins have diverse roles as electron carriers and redox enzymes in many biological processes. Their biological functions and electron transfer reactions are vigorously studied.[5] They are involved in most aspects of life including respiration, numerous steps of metabolism, photosynthesis, nitrogen fixation, nerve transmission, signal transduction, muscle contraction, oxygen transport and energy production.[2] The ability to understand and ultimately control the binding and activity of metals at protein sites is of great biological and medical importance. Metalloproteins are used in many experimental studies because of their favorable chemical and spectroscopic properties.[5]

Cytochrome *c*. Cytochromes are a class of proteins utilizing a metal cofactor called iron porphyrin (heme) to perform its biological function.[6] They are electron transfer enzymes supporting oxidative phosphorylation using the finely-tuned redox potential of iron complexed by the porphyrin ring.[7] Their heme prosthetic group is covalently attached to the protein's polypeptide backbone via two thioether linkages to cysteine residues (14 and 17).[8] This differentiates cytochrome *c* from other heme proteins (like hemoglobin and myoglobin) where the porphyrin is not covalently attached.[9] The preparation of H_2cyt, incorporation of metal ions into H_2cyt, and our reversible unfolding studies are much more complicated if the porphyrin ring is not covalently attached to the polypeptide backbone. In addition to the four nitrogens in the porphyrin ring, the heme iron is axially coordinated by two strong field protein ligands

(His 18 and Met 80).[10] The role of the heme moiety in the native conformation of cytochromes is still not completely understood.[8]

Cytochromes are highly conserved proteins across a spectrum of species found in plants, animals and many unicellular organisms.[6] It is a small globular protein with 104 amino acids found loosely bound to the inner membrane of mitochondria. The polypeptide chain is folded about the heme moiety forming a globular structure with a hydrophobic interior core and a hydrophilic exterior surface.[10] One of the important physical properties of cytochromes is the redox potential, which is the thermodynamic determinant for electron transfer and is also important in ligand binding.[7] The ready fluctuations of cytochrome *c* between ferrous and ferric states within the cell makes it an efficient biological electron transport shuttle, playing a vital role in cellular oxidation in both plants and animals. Cytochrome *c* is completely unfolded in the presence of denaturants, but is quantitatively refolded back to its native conformation upon removal of the denaturant.[10] It is hypothesized that the nonplanar distortions which are necessary for heme proteins to perform their biological role are maintained in the porphyrin of cytochrome *c* by a small protein segment which includes cysteines, the amino acids between the cysteine and the adjacent histidine ligands.[11] Hydrogen bonding within this segment is necessary to maintain the conformation of the peptide that induces the porphyrin distortion.[11] Experiments with native and carboxymethylated derivatives of cytochrome *c* indicate that only coordination with His 18 is necessary for the recovery of conformation and does not require a second ligand.[10] The well-characterized structural and thermodynamic properties of cytochrome *c* with highly soluble folded and unfolded forms makes it ideal for the study of structure function relationships of protein.[10] The

small size of cytochrome c, absence of disulfide bonds, its stability, and availability of various experimental methods to characterize the conformation of the protein in solution makes it an ideal model for the study of the mechanism of protein folding.[10]

Porphyrin Cytochrome c. Metal-free cytochrome c (H$_2$cyt), so-called porphyrin cytochrome c, has been previously prepared by selectively removing heme iron of cytochrome c using anhydrous hydrogen fluoride gas.[12] Porphyrin cytochrome c has a compact structure similar to that of native iron cytochrome c.[8] It exhibits the same viscosity, far UV circular dichroic and fluorescent properties.[12] However, it is more susceptible to denaturation by guanidine hydrochloride and by heat than native iron cytochrome c.[7] Important for our preparation of metal-substituted cytochromes, the removal of chemical denaturant allows H$_2$cyt (and the metal-substituted derivatives) to spontaneously refold. H$_2$cyt undergoes oxidative decomposition upon exposure to light; therefore exposure to light is minimized when working on this protein.[8]
H$_2$cyt competitively inhibits native iron cytochrome c in the cytochrome oxidase reaction.[13] It is also ineffective in restoring electron transfer in cytochrome c depleted mitochondria.[13] Like in iron cytochrome c, NMR studies confirmed the presence of thioether linkages between cysteine residues in the polypeptide backbone and the porphyrin ring in the H$_2$cyt.[9]

Neutral H$_2$cyt exhibits five absorbance maxima at wavelengths 404 nm, 505 nm, 539 nm, 567 nm and 619 nm.[12,14] This absorbance spectrum is characteristic of a porphyrin having two of its four pyrrole nitrogens protonated.[14] Removal of heme iron from iron cytochrome c to form H$_2$cyt relieves quenching of porphyrin fluorescence and enhances the fluorescence of the single tryptophan and four tyrosine groups.[14] Excitation

at 280 nm to obtain tryptophan fluorescence generates an emission spectrum with a maximum at 348 nm.[14]

As further proof of the importance of cofactors in the structural stability and folding of cytochromes, apocytochrome *c*, in which the thioether linkages are broken and the entire heme group removed, is completely unfolded under physiological conditions.[12]

Metal Substitution in Cytochrome *c*. Substitution of the iron ion in cytochrome *c* has been studied for many years, but little is still known about the overall impact of metal substitution on its properties, folding, structural stability, and biological function.[15,16] The study of metal-substituted cytochromes not only helps to better understand structure-function relationships, but also provides a deeper appreciation of why nature selected iron porphyrins as the prosthetic group in heme proteins.[7] In general, our research addresses why nature has specifically chosen a certain metal ion and if replacement of that metal ion by another leads to new structural properties and biological functions.

Iron is the central metal ion in heme proteins.[13] Metal substitution should shed light on whether the high activity and specificity of cytochromes in the biological reactions lies in the properties of the metal ion, lies in the characteristics of protein structure, or is an interplay of both.[13] Previous metal-substitution studies have shown manganese, cobalt, copper, zinc, nickel, and tin were capable of replacing iron in heme proteins. All the metal-substituted derivatives have characteristic absorption spectra which reflect their electronic properties.[13] Importantly, metal-substitution doesn't always lead to loss of biological function. It has been shown that the substitution of Fe^{2+} by Mn^{2+} in cytochrome c peroxidase preserves biological activity.[13] Cobalt cytochrome *c*

(Cocyt) is biologically active in the oxidation of cytochrome c oxidase.[13] Metal substitution often just alters the local coordination environment around the metal ion, leading to modest differences in structural and functional properties of metalloproteins.[7] Importantly, X-ray crystal structures as well as NMR solution structures have confirmed that metal-substitution only slightly perturbs the overall tertiary structure of cytochrome c.[8]

Many metal-substituted heme proteins exhibit fluorescence and phosphorescence which aids in the study of structure-functional relationship in heme proteins.[13] The fluorescence of metal-substituted cytochromes can provide information about protein:protein and protein:ligand interactions, such as the interaction between cytochrome c and its mitochondrial binding site.[17] Absorbance spectroscopy of metalloporphyrins has also been extensively used to follow protein conformational changes and chemical transformations.[18,19] Metal-substituted cytochromes can also help to better understand the role of metal ions in electron transfer enzymes and the effect of protein environment on the coordination chemistry of the metal ion.[20,21]

Kinetics and Mechanism of Metal Incorporation. Studying the kinetics of metal incorporation into porphyrins is helpful in understanding *in vivo* metal incorporation processes leading to natural metalloporphyrins and those found incorporated into proteins.[12,22] Different rates of formation for metalloporphyrins are also useful in comparing the properties of metal ions.[22] The mechanism of metal incorporation into a simple free porphyrin (let alone a porphyrin bound to the interior of a protein) can be a complex process with rates of incorporation several times slower than that of the complex formation of open chain ligands.[23] Metal ion incorporation into

porphyrins to form metalloporphyrins involves dissociation of two amine protons from the two pyrrole groups. This usually takes place in two steps.[22] First, coordination of the incoming metal ion with the two pyrrolenine nitrogens occurs to form an intermediate called the "sitting atop" complex (SAT).[24] The two protons on the pyrrole nitrogens still remain. Next, deprotonation of the SAT complex occurs, forming the metalloporphyrin.[22]

To facilitate incorporation of a metal ion, porphyrins have been observed to deform.[22,23,25] This deformation involves the movement of the four pyrrole nitrogens in upward and downward directions.[22,26] This conformation enhances the coordination ability of the lone pairs by directing them away from the central porphyrin cavity.[26] In N-substituted porphyrins where one of the hydrogen atoms bound to the pyrrole nitrogen is substituted with alkyl groups, a distorted structure due to the bulkiness of the group was observed.[22] This distorted structure has much faster metal ion incorporation rates compared to non-substituted porphyrins.[22] From these experiments it was deduced that the rate determining step in the metal ion incorporation is the dissociation of a coordinated solvent molecule from the metal ion in the outer-sphere associated complex and also deformation of the porphyrin ring prior to the rate determining step.[22]

The following is a summary of the various processes involved in metal ion incorporation into simple free porphyrins: distortion of the porphyrin ring, formation of an outer-sphere encounter complex, exchange of a bound solvent molecule with the first pyrrolenine nitrogen, closure of the chelate ring to form the SAT complex, deprotonation of the first pyrrole nitrogen in the SAT complex, and finally deprotonation of the second

pyrrole nitrogen to form the metalloporphyrin.[22] Formation of the SAT complex in simple metalloporphyrins was proven by spectroscopic and equilibrium data.[24]

The kinetics of metal ion incorporation into the porphyrin ring also depends on the metal ion.[4] The rate of metal ion incorporation is sensitive to the dissociation rate of coordinated solvent ligands which in turn depends on the oxidation state of the metal ions.[23] For example, copper(I) ions are more rapidly incorporated into porphyrin as compared to copper(II).[23] Large metal ions, such as mercury(II) and cadmium(II), cannot fit into the porphyrin opening and remain above the plane in the metalloporphyrin.[4] Therefore, this reaction is relatively fast and it proceeds through a pathway involving mononuclear-activated complexes.[4,22] Incorporation of medium-sized metal ions like cobalt(II) and copper(II) proceeds through the formation of homodinuclear-activated complexes.[4,22] In homodinuclear-activated complexes, the first metal ion is weakly bound to porphyrin, deforming the porphyrin ring and facilitating attack from the back of another metal ion.[4,22] This process is slow, and can proceed rapidly in the presence of large metal ions like mercury(II) or cadmium(II) through a heterodinuclear-activated complex in which two different metal ions bind to the porphyrin on opposite sides.[4,22,23] The large metal ions deform the porphyrin ring, facilitating attack of the smaller-sized metal ion from the opposite side.[4,23]

It is difficult to predict the reaction orders for metal ion incorporation reactions. Previous research shows that the kinetics of metal ion incorporation can be both first order with respect to the metal ion concentration and non-first order.[4,25,27] In a previous study, Zn^{2+} was incorporated into H_2cyt with second order reaction kinetics. The rate of incorporation is not limited by the penetration of the metal ion into the protein.[29]

The relative rates of incorporation for divalent metal ions is Cu > Zn > Co, Fe, Mn > Mg, Ni, which is similar to their rates of water exchange indicating the importance of desolvation of the metal ion before incorporation into the porphyrin.[30] Metal ions, once bound to the porphyrin, are slow to dissociate since deformation appears to be the main process rather than metal ion dissociation.[26]

Copper Cytochrome *c*. Copper cytochrome *c* (Cucyt) has been previously prepared via incorporation of a Cu^{2+} ion into H_2cyt and its incorporation is rapid when compared to other divalent metal ions.[26] In contrast to all other metal-substituted cytochromes, preparation of Cucyt results in an absorbance spectrum containing two heme Soret bands at 403 nm (Cucyt B) and 421 nm (Cucyt A). This indicates the formation of two spectroscopic forms.[20] It was also shown that the relative yields of the two forms depends primarily on the starting material (Fecyt) and was independent of other parameters like Cu^{2+} concentration, reaction time and reaction temperature.[20] The authors suggested that this may be due to heterogeneous cytochrome *c* conformational responses to Cu^{2+} ion substitution.[20] This lack of understanding of why two spectroscopic forms of Cucyt exist leads us to our current study.

The Cucyt A form has the same electrophoretic and ion exchange chromatographic mobility as the original iron cytochrome *c* indicating similar surface charges on the protein. However they may differ in distribution of charges and local structure. The Cucyt B form in comparison, has reduced elctrophoretic mobility. Circular dichroism in the UV region of Cucyt indicates a slightly altered protein confirmation, with a decrease in the α-helicity in comparison to the native Fecyt. These

conformational differences may be due to the displacement of peptide residues as a consequence of repulsion of axial ligands with antibonding d electrons in Cucyt.[20]

Both forms of Cucyt have absorbance spectra that depend on pH-induced conformational changes. The two forms at different pH values have electronic spectra characteristic of metalloporphyrins indicating that there is no dissociation of copper ion from the porphyrin ring.[20] The Cucyt A form at neutral pH has a heme Soret absorbance band at 422 nm. At both acidic and basic conditions (pH 2 and pH 13), the Soret band shifts to 390 nm.[21] These pH-dependent spectral changes are complicated by dimerization and changes in copper(II) coordination environment. At neutral pH, a heme Soret absorbance band at 422 nm is observed, indicating a monomeric and five-coordinate system. At extreme pH values, the heme Soret absorbance band shifted to 390 nm, indicating a dimeric and four-coordinate copper(II) ion. Free copper(II) porphyrins dimerize at extreme pH's with Cu–Cu distances of 4.2 Å. Earlier it was suggested that at neutral pH, large shifts in the heme Soret band (31 nm) were due to six-coordination, however no evidence was found to support this. At extreme pH values, the shift of 15 – 18 nm was suggested to be due to the π-π dimerization of Cu porphyrins, while the remaining shift is due to the axial ligation and its effect on porphyrin:metal interactions.[21] It is well-known that the position of the heme Soret absorbance band in metalloporphyrins depends on the axial ligation and the stereo-electronic interactions between the axial ligand and π electron system of the porphyrin.[20]

In comparison to other metal cytochromes (such as Fecyt), Cucyt was suggested to have two axial ligands.[20,21] His 18 and Met 80 were suggested as the 5th and 6th ligands, even though positive evidence was lacking.[20,21] High-resolution NMR

spectroscopic studies could not be done on Cucyt because of paramagnetic line broadening, so the identification of the axial ligands is still uncertain.[20,21] However EPR studies have been helpful in determining the coordination of Cu^{2+} ions.[21] The axial ligands in Cucyt were shown to be one nitrogen and one sulfur by paramagnetic resonance.[17]

Cucyt exhibits luminescence that is characteristic of copper(II) porphyrins and other metal-substituted cytochromes.[13,19] It shows a fluorescence emission spectrum maximum at 688 nm with shoulders at 715 nm and 762 nm.[19] The luminescence spectra of Cu porphyrins are temperature dependent with spectral shifts suggesting the existence of two excited forms.[17] Luminescence studies have been extremely helpful in the study of protein:protein interactions (for example cytochrome *c* with cytochrome *c* oxidase[17]) and Cucyt has also been used as a structurally faithful, redox-inert inhibitor probe in the mechanism of electron transfer between cytochrome *c* and cytochrome *c* peoxidase.[31] Although steady-state fluorescence spectroscopy has already been used to investigate Cucyt under limited conditions,[17,19] we will move beyond this research and determine the structural stability of Cucyt. To help us investigate structural stability, we will excite at 280 nm the single tryptophan found in cytochrome *c* and monitor the changes in fluorescence intensity at 331 nm as a function of denaturant concentration or temperature.

In summary, substitution of Cu^{2+} into porphyrin cytochrome *c* (H_2cyt) results in various conformational forms and the lack of understanding why these two spectroscopic forms of Cucyt exist leads us to study the purification and characterization of each Cucyt form.

Zinc Cytochrome *c*. Zinc cytochrome *c* (Zncyt) is prepared by incorporation of a Zn^{2+} ion into H_2cyt.[26] Previous spectroscopic and structural studies (NMR solution structures) of Zncyt show that metal incorporation does not alter the overall protein structure.[32] Zncyt has a Soret absorbance maximum at 423 nm and two other maxima in the α/β region at 549 nm and 585 nm. This characteristic absorbance spectrum of Zncyt will be used to study metal ion incorporation. Moreover, Zncyt exhibits fluorescence emission maxima at 560 nm and 640 nm. Therefore, Zncyt resembles other simple metalloporphyrins in their electronic absorption and emission properties.[13] The zinc(II) porphyrin in Zncyt is acid labile; incubation below pH 2 for 30 minutes at 25°C results in the release of Zn^{2+} and recovery of the free base porphyrin form.[13] This demetallation process was monitored spectrophotometrically with the appearance of the characteristic absorbance spectrum of H_2cyt containing four distinct maxima in the region of 500 – 650 nm. Zncyt is light sensitive (oxidative degradation of the porphyrin ring occurs) and care is taken during its preparation and use to ensure exposure to light is minimized.[13]

NMR structural studies have been performed to study the zinc(II) coordination environment in Zncyt. Previous spectroscopic and crystallographic studies on zinc(II) porphyrin model complexes showed zinc preferred pentacoordinate geometries. In the first NMR structural study, chemical shifts for His 18 and Met 80 were observed to be similar to that of the native iron cytochrome *c* which supported the proposal that zinc(II) is hexacoordinate with His 18 and Met 80 as the axial ligands. Chemical shifts of alternative ligands like His 33, Lys 79 and Phe 82 are the same as iron cytochrome *c*, excluding their possibility as the axial ligands to zinc(II).[33] The second NMR structural study also identified a hexacoordinate zinc(II), however the bond to Met 80 was

weakened.[34] In either case, it appears that the protein environment imposes a hexacoordinate geometry on zinc(II).

The ionic radius and charge of zinc(II) resemble iron(II).[33] In some disease conditions where iron metabolism is impaired, iron in heme proteins are substituted by zinc(II), suggesting the structure of zinc-substituted proteins is very close to normal iron derivatives.[33] Zncyt is used as an adequate structural model for iron cytochrome c as both share the same overall structure including axial ligands, environment in porphyrin vicinity and the same binding interface with redox partners.[33] Zncyt has been widely used in the study of protein-protein interactions and photo-induced electron transfer reactions between proteins.[34] Ground state and excited state redox behavior of Zncyt was studied with its oxidation potential and reaction rates calculated.[16] Studies of the kinetic reactions of both the excited state and the cation radical species show rapid reactivity with small molecular reagents.[16]

Substitution reactions of zinc(II) by copper(II) in zinc(II) porphyrin model complexes have been studied. It shows a first order dependence on copper(II) and zinc(II) porphyrin. The reaction was not retarded by zinc(II) and no evidence of intermediates was observed.[35]

Protein Folding and Unfolding. Proteins are the agents of biological function. They control all aspects of cellular metabolism, regulate movement of various ions across membranes, convert and store energy. Information to perform these biological functions is contained in the structure of the protein. All of the information necessary for folding the peptide chain into its native structure is contained in the amino acid sequence. Without acquiring its native, three-dimensional folded structure, the protein will remain

biologically inactive. Hydrogen bonds, hydrophobic interactions, electrostatic interactions and van der Waals interactions play an important role in the protein conformation and folding.

The intricate details of protein's structure can be resolved into different levels of organization. The primary structure is simply the amino acid sequence. Secondary structure is the local arrangement of a polypeptide chain into α-helices and β-sheets upon formation of hydrogen bonds. The polypeptide chain bends and folds to assume a tertiary structure, adopting a globular shape which gives lower surface to volume ratio, minimizing the interaction of the protein with the surrounding environment thus providing stability to the folded protein molecule. Quaternary structure (subunit organization) exists if two or more polypeptide chains interact.[1]

Proteins retain their native structure and function within a small range of environmental conditions. Under extreme conditions like high temperature or extreme acidic or basic pH, proteins undergo denaturation or unfolding by disruption of the weak noncovalent interactions essential for maintaining the structure of protein.[1] The study of protein structure in the presence of denaturants, at high temperatures or extreme acidic or basic pH is of great importance in understanding protein folding mechanisms. Partially unfolded forms are representatives of protein folding intermediates while fully unfolded forms resemble the conformation of a protein at the beginning of the protein folding process.[3] Protein unfolding occurs when the delicate balance of noncovalent interactions within the protein and with its aqueous environment are disrupted.[36] This leads to the destruction of secondary, tertiary and quaternary structure. The primary structure is retained (i.e. the covalent polypeptide backbone remains intact). However, upon the

removal of denaturing conditions, proteins regain their normal three-dimensional folded structure.[1]

Protein Denaturating Agents. Proteins are unfolded by extreme acidic and basic pH, various organic solvents, salts, detergents, chemical denaturants like urea and guanidine hydrochloride, and by high temperatures. High temperatures cause an increase in the kinetic energy and molecular vibrations resulting in the disruption of noncovalent interactions and unfolding of the protein. Thermal denaturation can be reversible or irreversible. Proteins are unfolded at acidic and basic pH values. Protein unfolding results from the ionization of amino acid side chains that are accessible to the solvent. High charge density causes electrostatic repulsion, destabilizing the native conformation. Organic solvents disrupt hydrogen bonds, hydrophobic interactions and electrostatic interactions. Organic Solvents function as proton donors or acceptors. Competition occurs between the protein and solvent hydrogen bonds, which in turn depends on the strength of hydrogen bonds between solvent molecules. Sometime organic solvents destabilize proteins and sometimes they actually favor the formation of hydrogen bonds within the protein, inducing a more globular structure for the protein. Organic solvents also affect hydrophobic interactions since nonpolar amino acid side chains are more soluble in organic solvents. The effect of solvents on electrostatic interactions is a function of their dielectric constant and may be either attractive (forming salt bridges and stabilizing protein structure) or repulsive (causing destabilization of the protein's native conformation). High concentrations of inorganic salts can induce conformational transitions in proteins by either attractive or repulsive electrostatic interactions, causing protein unfolding.[1]

Of particular importance for our work, urea and guanidine hydrochloride (GuHCl) are powerful protein denaturating agents. The exact mechanism by which they cause denaturation is not yet fully understood, but it seems that they interact directly with the protein, disrupting it, or indirectly by inducing changes in the aqueous solvent itself, or a combination of both.[38] The location of denaturant binding sites on the protein is also unclear. They may physically diffuse into the protein and interact directly with the polypeptide backbone and amino acid side chains, disrupting intramolecular hydrogen bonds and van der Waals interactions. They may also induce denaturation indirectly by disrupting the solvent environment, causing favorable water-protein interactions where water moves into the protein's hydrophobic core, destabilizing it.[36] In the presence of GuHCl, the globular proteins undergo conformational changes, unfolding it.[11] GuHCl mainly induces changes on the protein's surface, making water a better solvent for nonpolar amino acid side chains. On the other hand, urea disrupts hydrogen bonding both on the protein's surface and within its hydrophobic core.[39] On both the protein's surface and its hydrophobic core, urea interacts with various functional groups and denatures the protein by making nonpolar groups more soluble and altering water's structure and dynamics, introducing nonpolar groups to water and facilitating the exposure of amino acid residues in the protein's hydrophobic core.[39] In solution, GuHCl ionizes into guanidinium ions and chloride ions, disrupting electrostatic interactions within the protein, destabilizing it.[15] Urea being uncharged does not have an effect on the electrostatic interactions within proteins.[15] Both urea and GuHCl essentially affect the protein in similar ways, but they have different modes of action. In the literature, urea and GuHCl are used interchangeably in protein denaturation studies. However, recent

work has indicated that the intermediates and unfolded forms of these two denaturants may actually differ. Differences are mainly attributed to the ionic nature of GuHCl, although these differences may also extend beyond this ionic nature.[40] In contrast to the normal role of chemical denaturants, low concentrations of these denaturants can actually stabilize proteins below their denaturating concentrations. This stabilization is caused by crosslinking amino acids side chains within the protein, reducing its overall conformational dynamics.[41] The major advantage of denaturant-induced unfolding is that high reversibility can be maintained over extended periods of time.[6] For time dependent experiments like ours, this is extremely important.

Iron Cytochrome *c* Unfolding Studies. Vigorous research on iron cytochrome *c* shows it undergoes protein unfolding in the presence of various denaturants. The folding and unfolding of iron cytochrome *c* is strongly influenced by the binding of ligands to the iron in the covalently attached heme.[42] It undergoes highly reversible denaturation, unfolding in the presence of GuHCl and urea, but refolds back to its original conformation upon the removal of the denaturant.[10] In earlier NMR studies, denaturation by urea or GuHCl at neutral pH leads to the replacement of the native Met 80 axial ligand with one or more protein-donated strong field ligands or solvent water. The other axial ligand, His 18 remains coordinated to the heme iron.[42] Additional NMR structural studies have been carried out to more fully characterize the unfolding intermediates and completely unfolded iron cytochrome *c* in GuHCl.[40] Unfolded and partially unfolded species with non-native ligands to the heme iron were detected.[40] Two equilibrium unfolding intermediates with axial ligation of the heme iron by His and Lys and two unfolded species with axial ligation of the heme iron by His and His were detected.[43]

The structural and thermodynamic properties, as well as whether iron cytochrome c is stabilized by the presence of these non-native ligands is still not well known. More recent NMR studies have shown that the partially unfolded intermediates contain native-like structural features, such as an α-helical domain and solvent-shielded heme, but lacks the native Met 80 sulfur-heme iron linkage and shows many perturbations in amino acid side chains and other tertiary interactions.[43]

There are also differences in unfolding iron cytochrome c by GuHCl and urea. In GuHCl, two intermediates with heme iron axial ligation by His and Lys are observed upon partial denaturation, whereas only a single intermediate with heme iron axial ligation by His and Lys is observed with urea. This was explained by the ionic nature of the GuHCl.[40] Overall structural differences between the denatured states of urea and GuHCl are difficult to explain due to the absence of information about the structural contacts in the denatured state other than metal-ligand bonds.[40]

Partially-folded forms of proteins that exist at equilibrium under denaturating conditions (like the experiments we perform using GuHCl and urea) can provide information about the kinetic folding pathway of proteins. Proteins rapidly fold on the timescale of milliseconds to seconds and the intermediates that have been observed spectroscopically appear to be similar to the intermediates observed in equilibrium unfolding studies.[40] In the folding process of iron cytochrome c, an initial partially-folded intermediate was observed after 160 μs containing low native secondary structure (20% of the native form) while a second partially-folded intermediate was observed after 500 μs containing a larger content of native secondary structure (70% of the native form). After 15 ms, the completely-folded native form of cytochrome c was observed.[44] By understanding the

structural perturbations induced by equilibrium unfolding studies on cytochrome c, we can gain insight into the actual intermediates that appear during the protein folding process to better understand why proteins misfolding and their roles in protein misfolding diseases like scrapie, bovine spongi form encephalopathy (mad cow) and Alzheimer's disease.

As is the case for GuHCl-induced and urea-induced unfolding of iron cytochrome c, pH-induced conformational changes have also been well-studied. In iron cytochrome c at neutral pH, the heme iron axial ligands are Met 80 and His 18. At high pH (8-10), the dominant species is the so-called alkaline conformation in which Met 80 is replaced by a nearby Lys. Both the neutral pH and alkaline unfolded forms have a low spin heme, indicating that the heme iron's axial ligands are retained (even though the native Met is replaced by a non-native Lys). At acidic pH, the unfolded iron cytochrome c has a high spin heme, indicating that water has replaced the native protein-donated axial ligands.[6]

Zinc Cytochrome c Unfolding Studies. Although native iron cytochrome c has been vigorously studied, few protein unfolding studies have been carried out on the metal-substituted derivatives of cytochrome c.[5] GuHCl-induced unfolding of Zncyt produces changes in the Soret absorbance band (folded λ_{max} = 426 nm, unfolded λ_{max} = 418 nm).[45] During denaturation water molecules perturb the protein's porphyrin chromophore, leading to electrostatic contributions in the solvent shift counteracting the red shifting interactions.[46] Unfolding curves monitored via absorbance spectroscopy and circular dichroism show that the stability of folded Zncyt was similar to native iron cytochrome c.[5,45] As simple models, zinc(II) porphyrin complexes exhibit minimal aggregation in aqueous buffer.[47] Fluorescence line narrowing spectroscopy was used to

compare the folded and unfolded states of Zncyt.[48] Vibrational frequencies of Zncyt are perturbed upon denaturation.[48] Moreover, pressure-induced and temperature-induced unfolding of Zncyt were studied using fluorescence spectroscopy. It was inferred that electrostatic contributions prevail during the unfolding process. Conformational changes in Zncyt are caused at high pressures by forcing water into the protein pocket and at high temperatures as the protein interior gets exposed to water molecules.[46] The Zncyt protein folding rate is about 10 times faster than that of iron cytochrome c at comparable driving forces.[45] A heterogenous population of rapidly exchanging, roughly degenerate extended and compact non-native protein structures persist throughout the Zncyt unfolding process.[32]

Copper Cytochrome c Unfolding Studies. Although copper cytochrome c has been prepared and characterized in the fully folded form, no previous unfolding studies are known. There is ample opportunity to investigate partially and completely unfolding forms of copper cytochrome c, especially differences between Form A and Form B.

In this thesis, we will prepare H_2cyt, Zncyt and Cucyt. The conditions for metal-ion incorporation into H_2cyt varies from one metal to the next, so we will optimize the conditions for incorporation of zinc(II) or copper(II) into H_2cyt. To quantitatively determine the optimal conditions for incorporation, we will monitor this process via changes in the Soret absorbance over time. Using this data, we will determine the rates of incorporation of zinc(II) or copper(II) into H_2cyt as a function of temperature, concentration of metal ion, and concentration of chemical denaturant (urea and GuHCl). We will also investigate the incorporation of zinc(II) into H_2cyt to determine the lowest concentration of GuHCl that will induce conformational changes in H_2cyt that facilitate

incorporation. Finally, we will investigate the structural stability of Cucyt by monitoring changes in tryptophan fluorescence emission as a function of urea, GuHCl and temperature. The free energy for unfolding (ΔG_U) Cucyt will be obtained. Our work will provide insight into the kinetics and mechanism of metal-ion incorporation into H_2cyt and the stability of the metal-substituted cytochromes to better understand the role metal ions play in structure-function relationships.

CHAPTER 2.

MATERIALS AND METHODS

Chemicals. Distilled water was demineralized to a resistivity greater than 15 $\Omega M \cdot cm$ by a Milli–Q Water System. Chromatography gels were purchased from Sigma Chemical Co., Pharmacia, and Bio-Rad. Urea and GuHCl (electrophoresis grade) were purchased from Fisher Chemical Co. and used as received. Copper(II) chloride (99.99%) and zinc(II) acetate (99.99%) were purchased from Sigma Aldrich Co. All other chemicals were purchased from Fisher Chemical Co. and used as received.

Buffers. Phosphate buffers of 50 mM, 85 mM and 100 mM concentration were prepared fresh from solid salts of $Na_2HPO_4 \cdot 7H_2O$ and had pH values of 7.00 ± 0.05.

Proteins. Horse-heart iron cytochrome c was obtained from Sigma Chemical Co. Porphyrin cytochrome c (H_2cyt) is prepared from horse-heart iron cytochrome c by treatment with anhydrous hydrogen fluoride gas.[5] Upon addition of hydrogen fluoride, iron is removed from the porphyrin ring in cytochrome c. Excess hydrogen fluoride is evaporated using nitrogen gas and the resulting viscous purple protein solutions is treated with 100 mM phosphate buffer pH 7 and 10 mM EDTA. This protein solution is applied to a spin desalting column and centrifuged to recover a dark purple solution of H_2cyt.

Prepared H_2cyt is purified using ion exchange and gel filtration chromatography to ensure the complete removal of any contaminating metal ions or degraded forms of protein present after the addition of hydrogen fluoride. Cation exchange chromatography is performed using CM Sepharose. First, the column (~15 mL column bed) is equilibrated using 50 mM phosphate buffer pH 7.0, protein is applied, and then 85 mM phosphate buffer pH 7.0 is used to elute the H_2cyt off the column, whereas the metal ions

and other degraded forms of the protein remain bound to the column. The whole process is carried out in dark.

If further purification of H_2cyt is required, gel-filtration chromatography using Sephedex G50 is performed. The column (~75 mL) is equilibrated using a solution containing 50 mM phosphate buffer pH 7.0 and 100 mM sodium chloride to prevent protein adsorption to the gel filtration column.

The obtained H_2cyt is concentrated using ultrafiltration using both Amicon stirred ultrafiltration cells (50 ml) and Amicon ultracentrifugal filter devices (4 ml). The concentration of purified H_2cyt was determined spectrophotometrically; the molar absorptivity of H_2cyt at 404 nm is 160 mM^{-1}cm^{-1}.[5]

Copper cytochrome c (Cucyt) was prepared by incubating unfolded H_2cyt with a ten-fold excess of copper(II) chloride.[26] H_2cyt is unfolded/denatured using 4.0 M GuHCl and incubated for 1 hour at 50°C in a water bath. Complete incorporation of Cu^{2+} into H_2cyt was confirmed spectrophotometrically. Dialysis into milliQ water is done to decrease the concentration of GuHCl and refold the protein (confirmed spectrophotometrically). Concentration of the protein solution is performed as above using an Amicon ultracentrifugal filter device. The concentration of prepared Cucyt is determined spectrophotometrically; the molar absorptivity of Cucyt at 542.5 nm is 12.9 mM^{-1}cm^{-1}.

Zinc cytochrome c (Zncyt) was prepared by incubating unfolded H_2cyt with a ten-fold excess of zinc(II) acetate.[5] H_2cyt is unfolded/denatured using 4.5 M GuHCl solution and incubated for 1 hour at 50°C in a water bath. Complete incorporation of Zn^{2+} in H_2cyt was confirmed spectrophotometrically. Dialysis into millQ water is done to

decrease the concentration of GuHCl and refold the protein (confirmed

spectrophotometrically). Concentration of the protein is performed as above using an

Amicon ultracentrifugal filter device. The concentration of prepared Zncyt is determined

spectrophotometrically; the molar absorptivity of Zncyt at 423 nm (characteristic Soret

absorbance band) is 243 mM^{-1}cm^{-1}.

Preparation of Denaturant Solutions. Solutions of different concentrations of

urea (1.0 M, 2.0 M, 3.0 M, 4.0 M, 5.0 M, 6.0 M, 7.0 M and 8.0 M) were prepared fresh

by a published procedure.[49] The actual concentration of each urea solution is measured

using a refractometer and the equation 1 is used to calculate the actual concentration of

GuHCl where $\Delta\eta$ is the difference in the refractive index of denaturant solution and

water.[49]

$$117.66(\Delta\eta) + 29.753(\Delta\eta)^2 + 85.56(\Delta\eta)^3 \tag{1}$$

The same procedure is also followed for the preparation of different

concentrations of GuHCl (0.5 M, 1.0 M, 1.5 M, 2.0 M, 2.5 M, 3.0 M, 3.5 Mand 4.0 M).

The actual concentration of each GuHCl solution is measured using a refractometer.

Equation 2 is used to calculate the actual concentration of GuHCl where $\Delta\eta$ is the

difference in the refractive index of denaturant solution and water.[49]

$$57.147(\Delta\eta) + 38.68(\Delta\eta)^2 - 91.60(\Delta\eta)^3 \tag{2}$$

UV-Vis Absorbance Spectroscopy. Absorbance spectroscopy is the

measurement of the intensity of the absorption of light in the UV and visible regions of

the protein. H$_2$cyt and metal-substituted cytochromes have different absorbance spectra

which forms the basis of our studies. All absorbance spectra were collected from 300 nm

to 800 nm. The absorbance spectra of our proteins were recorded with Shimadzu UV-

VIS-NIR Recording Spectrophotometer (Model UV-3100). A 1-cm quartz cell with a 1.5-mL volume was used. Temperature is controlled using a peltier temperature controller (CPS Controller-260). A computer and UV probe software allows for kinetic measurements and automatic collection of multiple spectra at various time intervals. Slit width was 2 nm.

Fluorescence Spectroscopy. Structural stability studies of Cucyt were done using fluorescence spectroscopy. The tryptophan emission spectrum of Cucyt changes as a function of denaturant which is the basis for our studies. Fluorescence spectra of Cucyt were recorded with an Aminco Bowman Series 2 Luminescence Spectrophotometer using a 1-cm quartz fluorescence cuvette with a 3-mL volume. Temperature is controlled using an external temperature bath (VWR Scientific). Excitation wavelength was set to 280 nm (to excite the one tryptophan (residue 59) found in cytochrome c) and fluorescence emission was recorded from 300 to 800 nm. Scan speed was 5 nm/sec.

Metal Ion Contamination in Porphyrin Cytochrome c Monitored by Heme Soret Absorbance. Denaturation studies of H_2cyt in the presence of GuHCl were performed to investigate the possible contamination of the prepared H_2cyt and also the effect of concentration of denaturant on conformational stability of protein. Denaturation of H_2cyt was monitored by following the change in the Soret absorbance at 404 nm as a function of GuHCl concentration (0.0001 M – 4 M). The cell compartment was maintained at 25.0±0.1°C. The concentration of H_2cyt used for each experiment was 7.5 μM to ensure a good signal-to-noise ratio. In some preparations of H_2cyt, contaminating metal ion incorporation was evident. Control experiments to determine the level of contamination were performed by incubating H_2cyt with decreasing concentrations of

denaturant (GuHCl) and monitoring the change in the Soret absorbance at 404 nm. These experiments serve the purpose of determining the lowest concentration of GuHCl that does not cause any changes in the protein conformation.

Incorporation of Zinc into H$_2$cyt as a Function of GuHCl and Urea. The preparation and the rate of incorporation of Zn^{2+} into H$_2$cyt were studied at different concentrations of urea (1.0 M – 8.0 M) and GuHCl (0.5 M – 4.0 M). Each of the incorporations was studied over a period of time depending on how rapidly the Zn^{2+} was incorporated. The cell compartment was maintained at 25±0.1°C. The concentration of H$_2$cyt used for the experiment was 7.5 μM. First, H$_2$cyt was pipetted into the denaturant solution in a 1-cm quartz cuvette and placed in the cell compartment of the spectrophotometer to equilibrate. After ten minutes, 13-fold excess of zinc(II) acetate is added (100 μM) to the cuvette solution. Incorporation/preparation of Zncyt was monitored via changes in the Soret absorbance at 404 nm (loss of H$_2$cyt) and 423 nm (formation of Zncyt). Twenty absorbance spectra were taken at various time intervals depending on the rate of zinc incorporation. At higher concentrations denaturation is faster, so in the case of 0.5 M, 1.0 M, 1.5M and 2.0 M GuHCl and 1.0 M, 2.0 M, 3.0 M and 4.0 M urea, spectra are collected every ten minutes, at 2.5 M GuHCl and 5.0 M urea, it was eight minutes, at 3.0 M and 3.5 M GuHCl and 6.0 M and 7.0 M urea, it was five minutes, and finally at 4.0 M GuHCl and 8.0 M urea spectra are collected every three minutes. The absorbance data at 404 nm and 423 nm are collected and exported into SigmaPlot for kinetic analysis.

Incorporation of Copper into H$_2$cyt as a Function of Temperature. To facilitate the unfolding of H$_2$cyt and the rate of incorporation of Cu^{2+} into H$_2$cyt,

temperature was increased. Incorporation of Cu^{2+} into H_2cyt was studied at 40°C, 45°C, 50°C and 55°C. These experiments were also studied over various time periods. The concentration of H_2cyt used for the experiments was 7.5 μM. First, H_2cyt was pipetted into the denaturant solution in a 1-cm quartz cuvette and placed in cell compartment of spectrophotometer to equilibrate to the desired temperature. After ten minutes, 13-fold excess of $CuCl_2$ is added (100 μM) to the cuvette solution. Incorporation of Cu^{2+} was monitored by changes in Soret absorbance from 404 nm (loss of H_2cyt) to 422 nm (formation of Cucyt). Twenty spectra are collected at various time intervals. At higher temperatures denaturation is fast, so at 40°C, spectra are collected for every ten minutes, at 45°C, spectra are collected for every five minutes and at 50°C and 55°C, spectra are collected for every two and three minutes respectively. The absorbance data at 404 nm and 422 nm are collected and treated as described below.

Incorporation of Copper into H_2cyt as a Function of Guanidine Hydrochloride. Preparation and rate of incorporation of Cu^{2+} in H_2cyt were studied using different concentrations (0.5 M – 4.0 M) of GuHCl. These experiments were also studied over various time periods. The cell compartment was maintained at 25±0.1°C. The concentration of H_2cyt was 7.5 μM and $CuCl_2$ was 100 μM (13-fold excess of Cu^{2+}). Incorporation was monitored by changes in Soret absorbance at 404 nm (loss of H_2cyt) and 390 nm and 422 nm (formation of two different forms of Cucyt). Twenty spectra are collected at various time intervals. At higher concentrations of GuHCl incorporation is fast, so at 0.5 M are collected for every fifteen minutes, at 1.0 M, 1.5 M, 2.0 M GuHCl, spectra are collected for every ten minutes, at 2.5M GuHCl, spectra were collected every eight minutes, at 3.0 M and 3.5 M GuHCl, spectra were collected every five minutes, and

finally at 4.0 M GuHCl, spectra were collected for every three minutes. These

experiments were repeated, however, the time interval between each spectrum was

decreased so the rapid incorporation of Cu^{2+} can be more closely studied at shorter time

intervals with a greater number of data points. The absorbance data at 390 nm, 404 nm

and 422 nm are collected and treated as described below.

Kinetics of Metal Incorporation. The collected absorbance data were fitted

using nonlinear least-squares regression in SigmaPlot, Version 8.0 (Systat Software).

The absorbance at 404 nm (characteristic of H_2cyt) decreases and the absorbance at ~420

nm (characteristic of metal-incorporated cytochrome c) increases. The rate constants

were obtained from changes in Soret absorbance at 404 nm and 423 nm. The rate

constants for the loss of H_2cyt and the formation of metal-substituted cytochrome c were

obtained using the following equations for exponential decay of H_2cyt (equation 3) and

exponential rise to maximum of meta-substituted cytochrome c (equation 4). Exponential

$$y = y_0 + ae^{-k_d x} \qquad (3)$$

$$y = y_0 + a\left(1 - e^{-k_f x}\right) \qquad (4)$$

decay of H_2cyt at 404 nm and the exponential rise to maximum of Zncyt at 423 nm was

fitted using Sigma Plot 8.0. The rate constants for decay of H_2cyt (k_d) were obtained

using equation 3. The rate constants for formation of Zncyt (k_f) were obtained using the

equation 4.

In case of Cucyt at low denaturant concentrations, formation of two forms of

Cucyt was observed with Soret absorbance bands at 403 nm and 422 nm. Only one form

of Cucyt was observed at higher concentrations with a Soret absorbance band at 390 nm.

The rate constants were obtained from changes in Soret absorbance at 390 nm, 404 nm

and 422 nm using nonlinear-least squares regression (Sigma Plot, version 8.0 from Systat Software). The rate constants for decay of H_2cyt were obtained using the equation 3. The rate constants for formation of Cucyt were obtained using the equation 4.

Equilibrium Unfolding of Cucyt Monitored by Tryptophan Fluorescence.

Equilibrium unfolding of Cucyt as a function of denaturant and time were measured using fluorescence spectroscopy. Cytochrome *c* contains a single tryptophan (residue 59) that can be used to monitor overall structural stability. The excitation wavelength was set to 280 nm. The unfolding of Cucyt at increasing concentrations of GuHCl (0.25 M – 4.5 M) and urea (0.25 M - 8.0 M) was monitored by the change in fluorescence emission in the region of 300 to 800 nm. Sensitivity of the instrument was set to 60% (photomultiplier tube voltage of 880 V) using the highest denaturant concentration (4.5 M GuHCl and 8.0 M urea) and remained the same throughout the experiment. The concentration of Cucyt used was 0.1 µM. Cucyt denaturant solutions were incubated and emission spectra were recorded after 4 hrs and 24 hrs. Fluorescence emission intensity at 331 nm was recorded as function of denaturant concentration since this is the wavelength where maximal change from the folded to unfolded Cucyt occurs. The data are analyzed as described below.

Fluorescence intensity at 331 nm was plotted against concentration of denaturant urea (0.25 M – 8.0 M) and GuHCl (0.25 M – 4.5 M) and fitted using a four parameter sigmoidal curve to obtain the midpoint of the unfolding transition (C_m). The fraction of unfolded Cucyt (F_U) and free energy for unfolding (ΔG_U) are calculated using the equation 5.

$$\Delta G_U = -RT \ln\left[\frac{y - y_F}{y_U - y}\right] \qquad (5)$$

CHAPTER 3.

RESULTS

Metal Ion Contamination in Porphyrin Cytochrome *c* Monitored by Heme Soret Absorbance. These are control experiments to study metal ion contamination in some preparations of H_2cyt. The contamination studies were done in the presence of different concentrations (0.0001 M – 4.0 M) of GuHCl. These are also used to quantify the lowest concentration of GuHCl that does not allow the incorporation of the contaminated metal ion into the H_2cyt. At very low concentrations (0.0001 M) of GuHCl, no change in the absorbance spectrum is observed (**Figure 1**). Therefore, there is no incorporation of any contaminating metal ion. At low concentrations (0.1 M), there is a shift in the Soret absorbance band over time indicating partial incorporation of a contaminating metal ion (**Figure 2**). Two distinct Soret bands are observed indicating a mixture of H_2cyt and a metal-substituted H_2cyt. At intermediate (0.5 M) concentrations there is complete incorporation which is a slow process with a very gradual shift in the Soret absorbance band over time; also the change in the region of 500 to 650 nm from four absorbance maxima to two, specifically the decrease in absorbance at 506 nm is indicative of complete incorporation of metal ion into H_2cyt (**Figure 3**). At higher concentrations (2.5 M) the incorporation was very fast taking about 24 minutes for complete incorporation of contaminated metal ion with an immediate shift in the Soret absorbance band and significant decrease in the absorbance at 506 nm which is indicative of the incorporation of metal ion into H_2cyt (**Figure 4**).
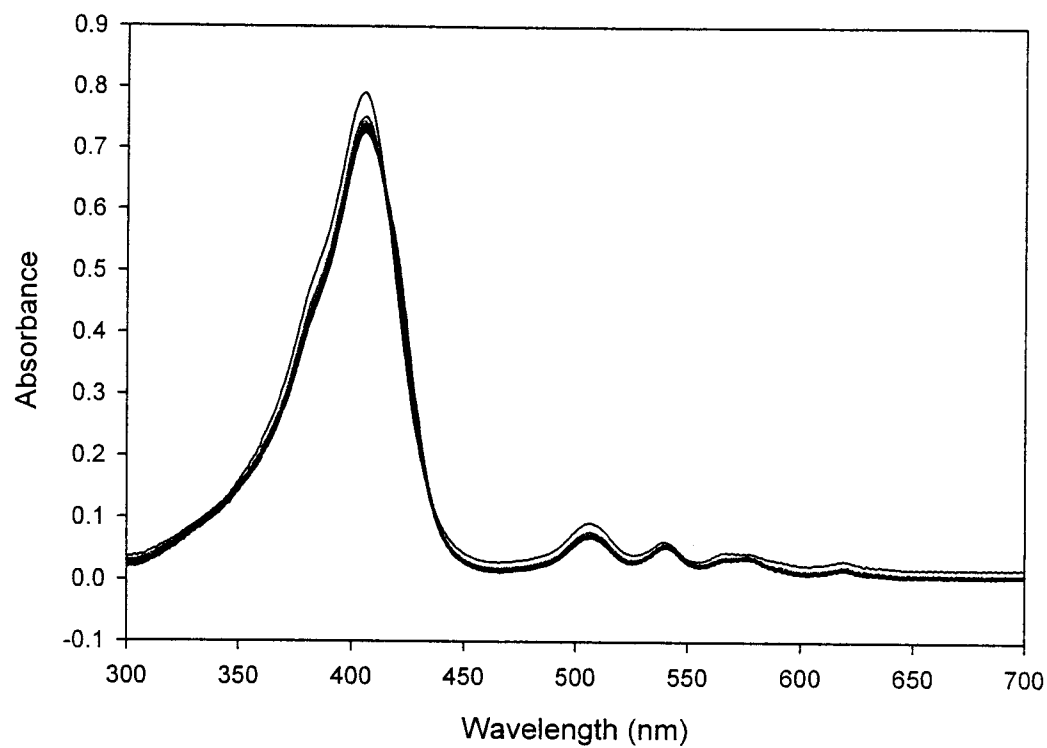
Figure 1. Lack of contaminating metal ion incorporation into H$_2$cyt at very low concentrations of GuHCl. Absorbance spectra collected over time of 7.5 μM H$_2$cyt dissolved in 0.0001 M GuHCl at 25°C. 20 spectra are collected at a time interval of 40 minutes for a total of 1960 minutes.

Figure 2. Contaminating metal ion incorporation into H₂cyt at low concentrations of GuHCl. Absorbance spectra of 7.5 μM H₂cyt collected over time in the presence of 0.1 M GuHCl at 25°C. Changes observed in the absorbance spectrum are due to unknown contaminating metal ion. 20 spectra are collected at a time interval of 15 minutes for a total of 285 minutes.
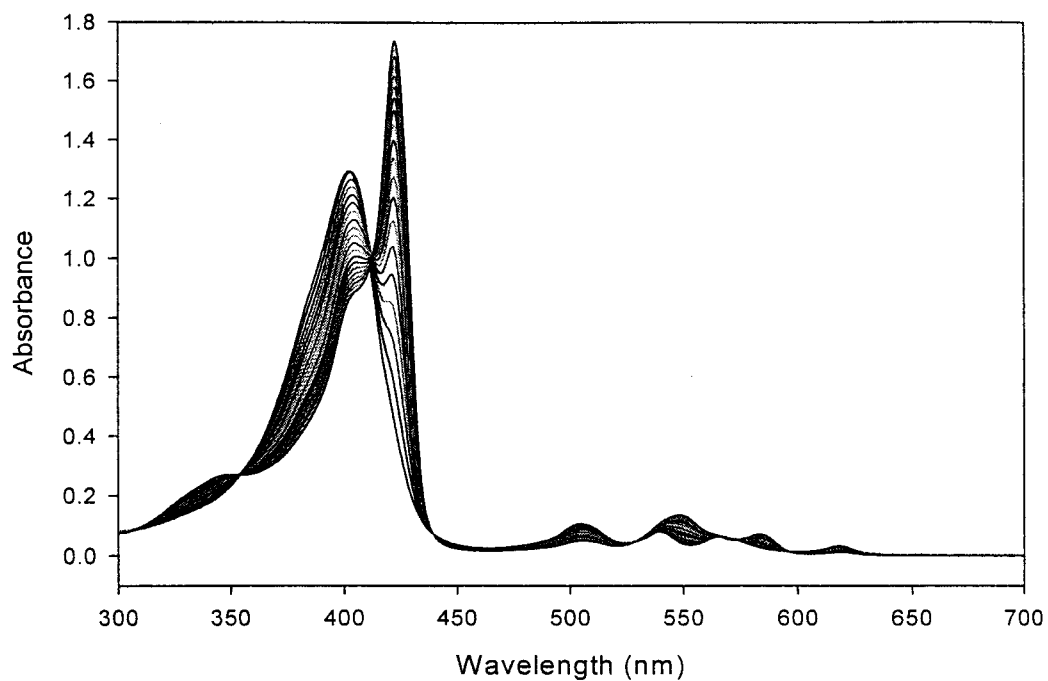
Figure 3. Contaminating metal ion incorporation into H₂cyt at intermediate concentrations of GuHCl. Absorbance spectra of 7.5 μM H₂cyt collected over time in the presence of 0.5 M GuHCl at 25°C. Changes observed in the absorbance spectrum are due to unknown contaminating metal ion. 20 spectra are collected at a time interval of 15 minutes for a total of 285 minutes.
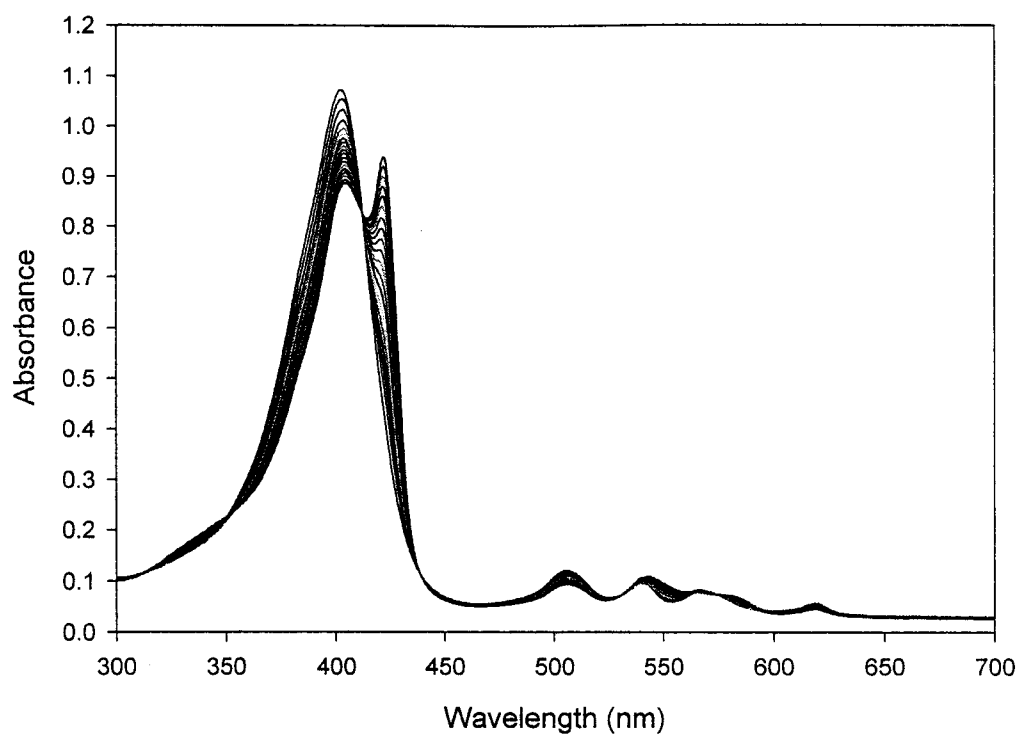
Figure 4. Contaminating metal ion incorporation into H₂cyt at high concentrations of GuHCl. Absorbance spectra of 7.5 μM H₂cyt collected over time in the presence of 2.5 M GuHCl at 25°C. Changes observed in the absorbance spectrum are due to unknown contaminating metal ion. 20 spectra are collected at a time interval of 8 minutes for a total of 152 minutes.
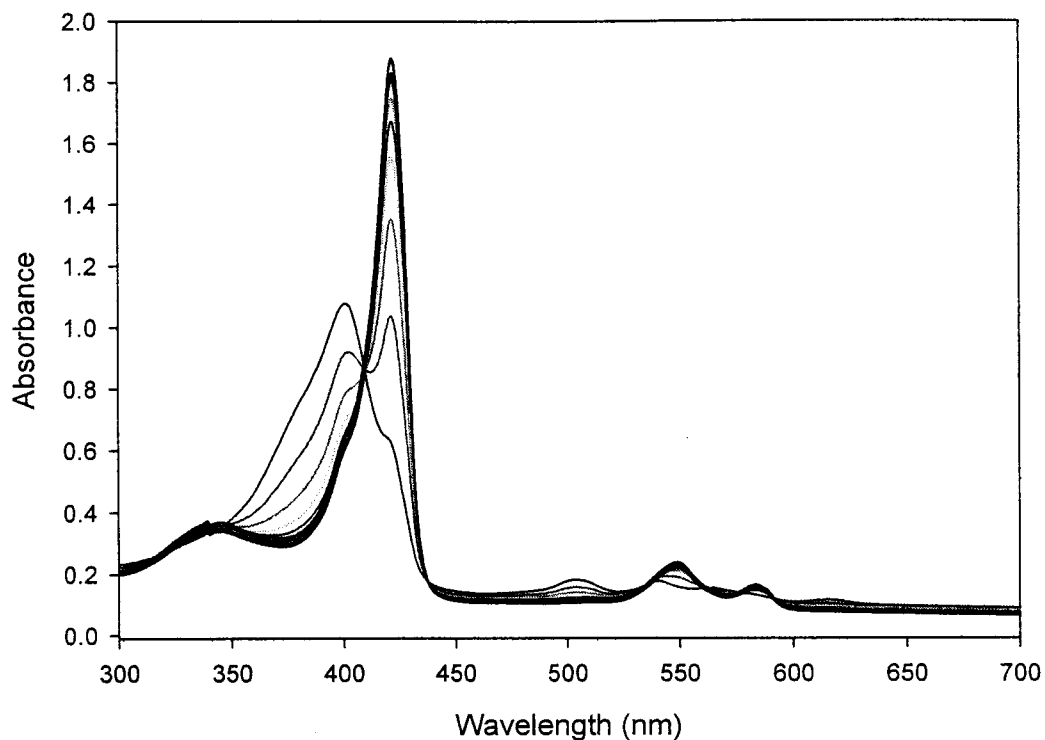
Incorporation of Zinc into H₂cyt as a Function of GuHCl. The complete

incorporation of Zn^{2+} into H₂cyt forming Zncyt is shown by the shift in Soret absorbance

band from 404 nm (characteristic of H₂cyt) to 423 nm (characteristic of Zncyt) and also

the change in the region of 500 to 650 nm from four absorbance maxima to two.

Specifically the decrease in absorbance at 506 nm is indicative of complete incorporation

of Zn^{2+} into H₂cyt. The Zncyt absorbance maxima are 423 nm, 540 nm and 580 nm.

Incorporation of Zn^{+2} in the H₂cyt was studied at different concentrations (0.5 M

– 4 M) of GuHCl. At lower concentrations (0.5 M), the incorporation was a slow process

with a very gradual red shift in the Soret absorbance band over time, leading to the

presence of two distinct Soret bands indicating a mixture of H₂cyt and Zncyt (**Figure 5**).

At intermediate concentrations (2.5 M), the incorporation was fast, within only a few

minutes the Soret absorbance band shifted from 404 nm to 423 nm (**Figure 6**). At higher

concentrations (4.0 M) the incorporation was very fast, so that the conversion from H₂cyt

to Zncyt could not be observed in the short time from placing the cuvette in the sample

chamber and starting the collection of spectra (**Figure 7**).

Figure 5. Zinc incorporation at low concentrations of GuHCl. Absorbance spectra collected over time upon incorporation of Zn^{2+} into 7.5 μM H_2cyt in the presence of 0.5 M GuHCl at 25°C. The concentration of Zn^{2+} is 100 μM. 20 spectra are collected at a time interval of 10 minutes for a total of 190 minutes.

Figure 6. Zinc incorporation at intermediate concentrations of GuHCl. Absorbance spectra collected over time upon incorporation of Zn^{2+} into 7.5 μM H_2cyt in the presence of 2.5 M GuHCl at 25°C. The concentration of Zn^{2+} is 100 μM. 20 spectra are collected at a time interval of 5 minutes for a total of 95 minutes.
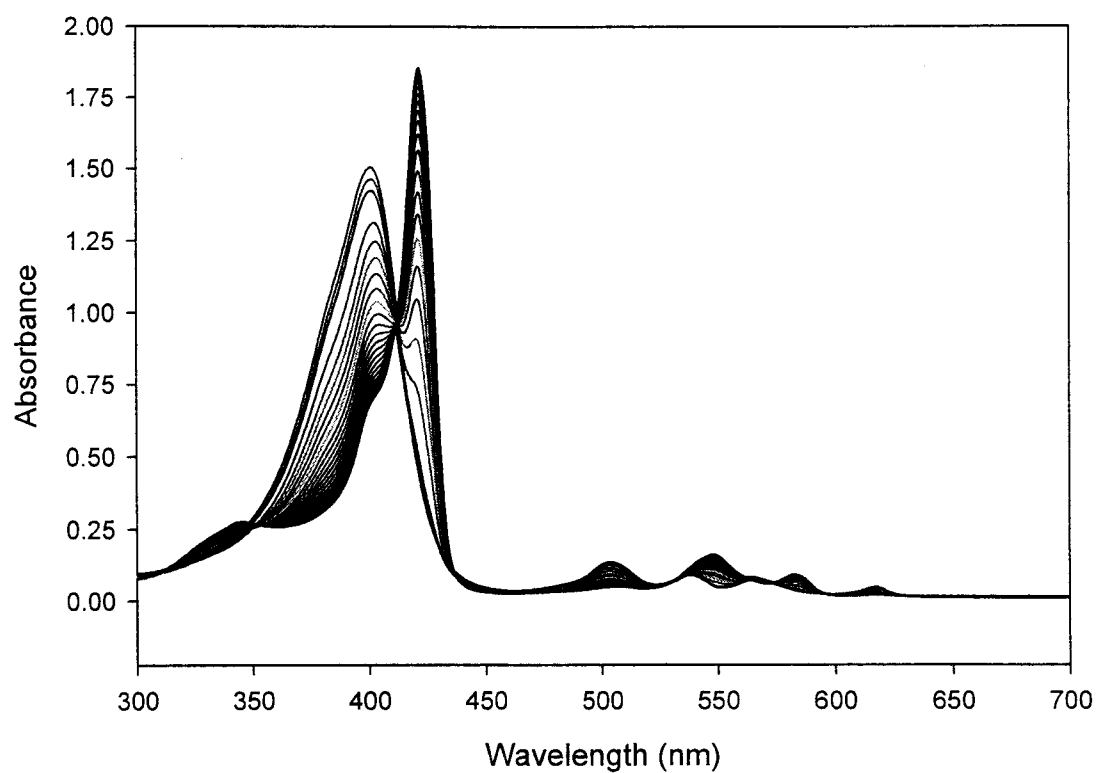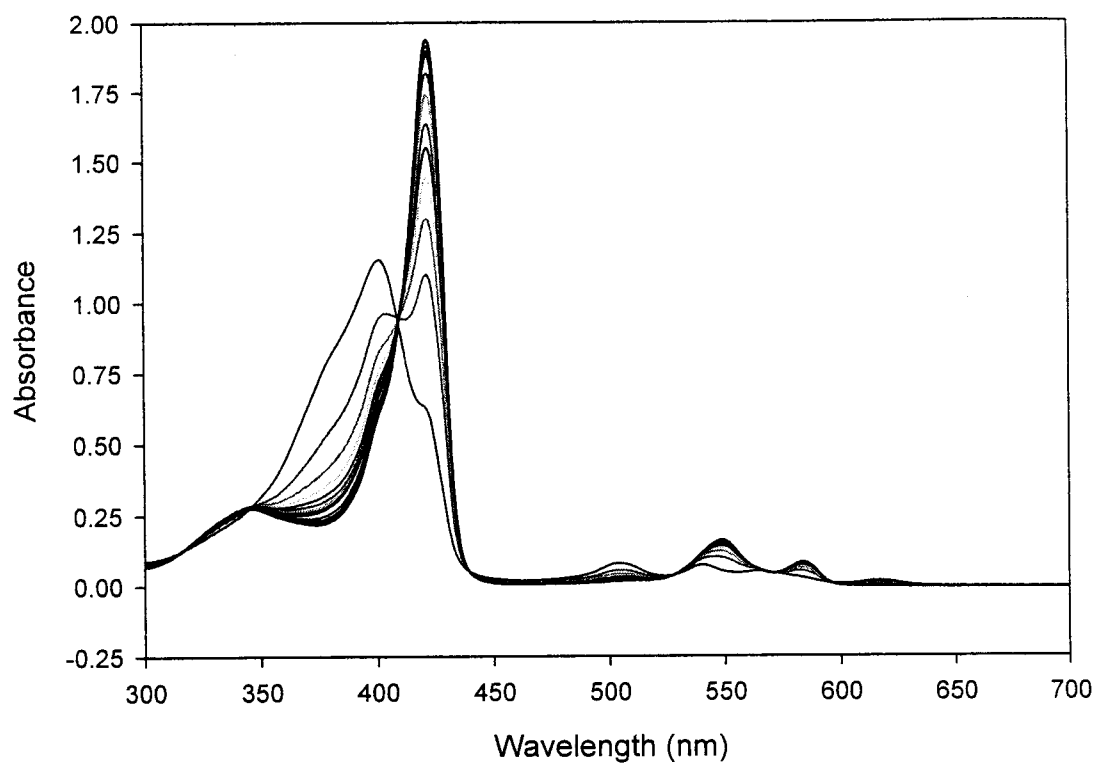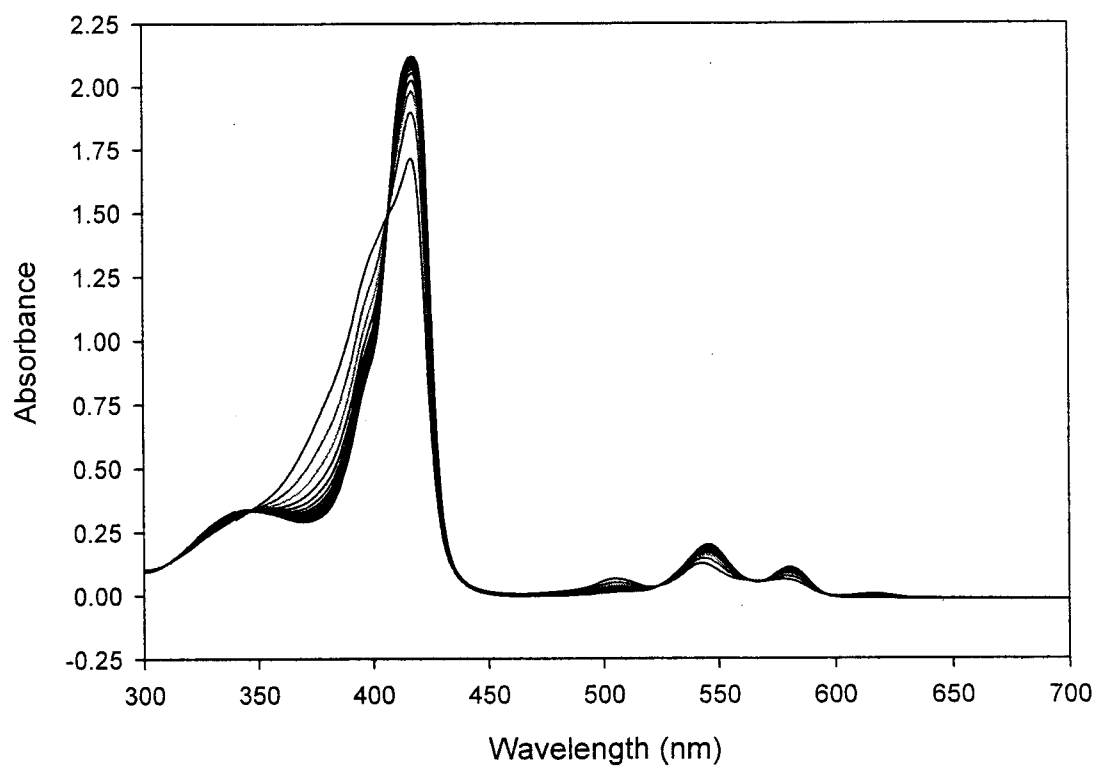
Figure 7. Zinc incorporation at high concentrations of GuHCl.
Absorbance spectra collected over time upon incorporation of Zn^{2+} into 7.5 μM H_2cyt in the presence of 4.0 M GuHCl at 25°C. The concentration of Zn^{2+} is 100 μM. 20 spectra are collected at a time interval of 3 minutes for a total of 57 minutes.

Rate constants for the incorporations of Zn^{2+} in the H_2cyt were obtained from the changes in the absorbance at 404 nm and 423 nm. At lower concentrations of GuHCl (0.5 M) where the incorporation was slow, the absorbance spectra show a gradual decay at 404 nm and gradual exponential rise at 423 nm. It takes about 180 minutes for complete incorporation (**Figure 8**). The rate constants for the decay (0.010 min^{-1}) and rise (0.014 min^{-1}) are nearly identical indicating that the conversion of H_2cyt to Zncyt takes place without the formation of any intermediates. Isobestic points in **Figures 5, 6, and 7**support this conclusion as well.

At higher concentrations of GuHCl (2.5 M – 4.0 M) incorporation were fast. It takes about 55 minutes and 40 minutes at 2.5 M and 4.0 M GuHCl, respectively. Due to the rapid incorporation of Zn^{2+}, only a few data points can be fitted to obtain the rate constants (**Figures 9 & 10**).

Figure 8. Rate constant plots for zinc incorporation at low concentrations of GuHCl. Change in heme Soret absorbance over time as Zn^{+2} is incorporated into H_2cyt in the presence of 0.5 M GuHCl. Data points for the exponential decay at 404 nm and the exponential rise at 423 nm were plotted. Rate constants were obtained by fitting the data to monoexponential equations (equations 3 & 4 in the Materials and Methods Section) using SigmaPlot 8.0. Experimental conditions: 7.5 μM H_2cyt, 25°C, 100 μM Zn^{2+}. The error reported for rate constants k_d and k_f are the standard deviation for the fitting.
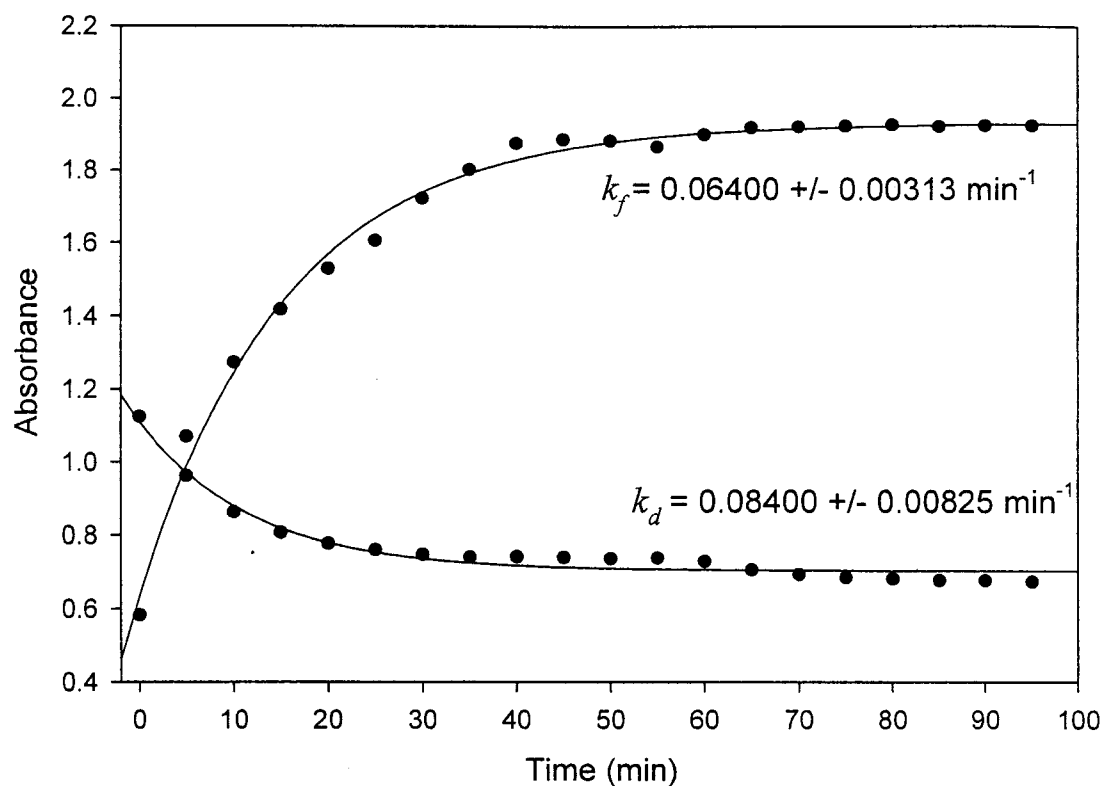
Figure 9. Rate constant plots for zinc incorporation at intermediate concentrations of GuHCl. Change in heme Soret absorbance over time as Zn^{+2} is incorporated into H_2cyt in the presence of 2.5 M GuHCl. Data points for the exponential decay at 404 nm and the exponential rise at 423 nm were plotted. Rate constants were obtained by fitting the data to monoexponential equations (equations 3 & 4 in the Materials and Methods Section) using SigmaPlot 8.0. Experimental conditions: 7.5 μM H_2cyt, 25°C, 100 μM Zn^{2+}. The error reported for rate constants k_d and k_f are the standard deviation for the fitting.
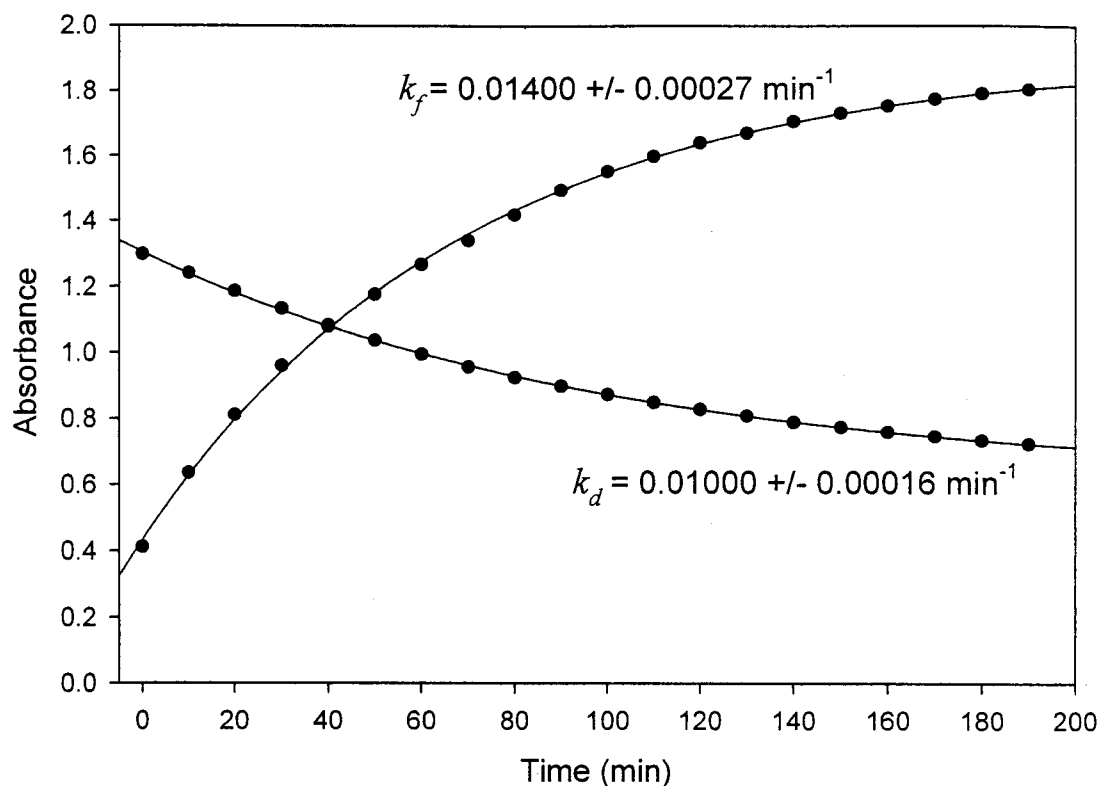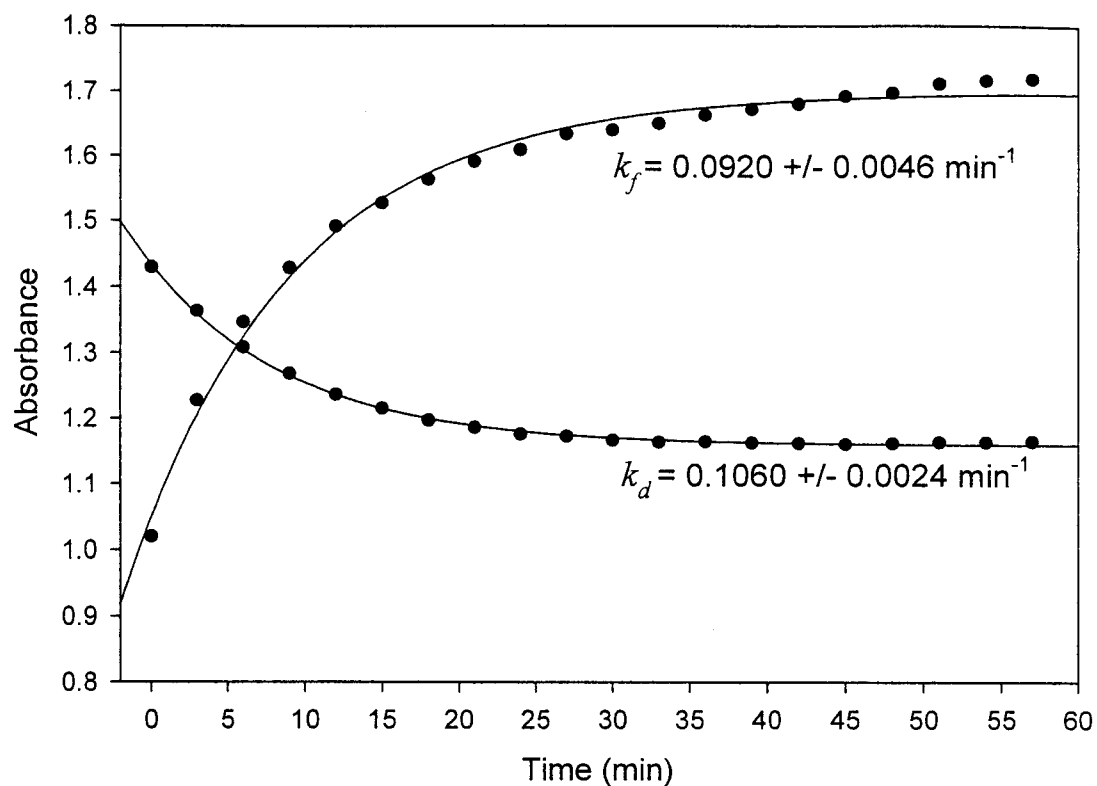
Figure 10. Rate constant plots for zinc incorporation at high concentrations of GuHCl. Change in heme Soret absorbance over time as Zn^{+2} is incorporated into H_2cyt in the presence of 4.0 M GuHCl. Data points for the exponential decay at 404 nm and the exponential rise at 423 nm were plotted. Rate constants were obtained by fitting the data to monoexponential equations (equations 3 & 4 in the Materials and Methods Section) using SigmaPlot 8.0. Experimental conditions: 7.5 µM H_2cyt, 25°C, 100 µM Zn^{2+}. The error reported for rate constants k_d and k_f are the standard deviation for the fitting.

Rate constants for the disappearance of H_2cyt at 404 nm upon incorporation of Zn^{2+} into H_2cyt as a function of GuHCl concentration (0.5 M – 4.0 M) were obtained. With the increase in GuHCl concentration, the rate constants also increased but appear to plateau above 2.0 M concentration (**Figure 11**). It clearly shows that GuHCl concentrations as low as 2.0 M provide optimal Zn^{2+} incorporation into H_2cyt.
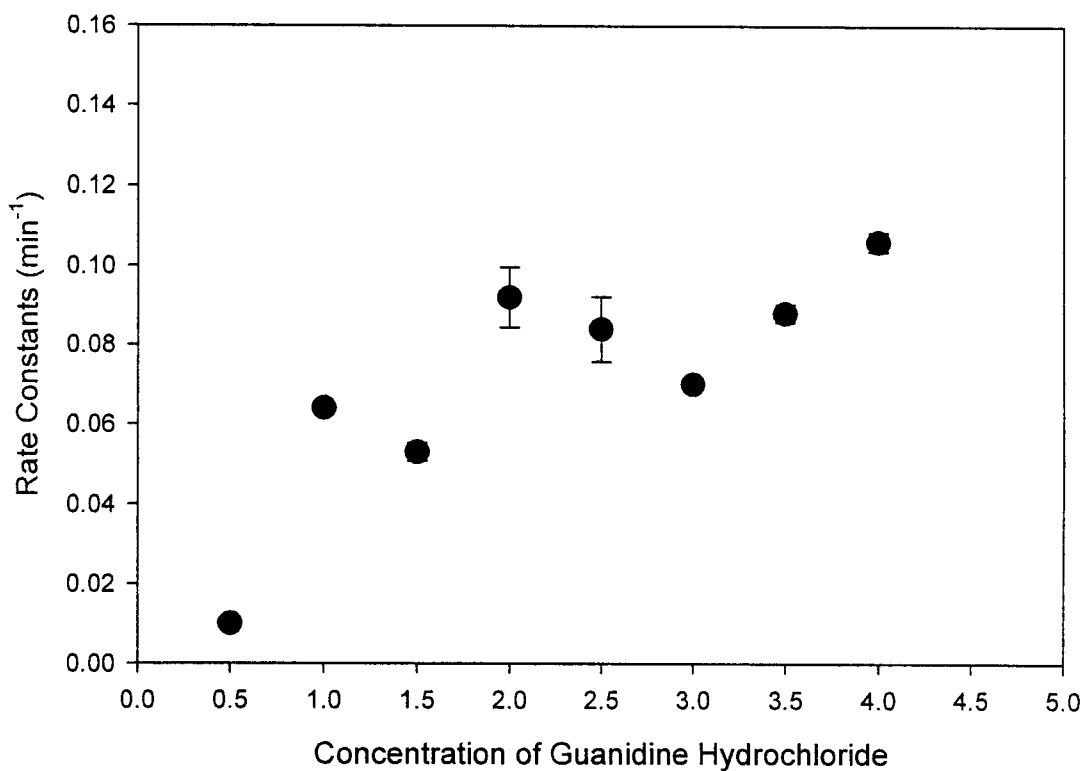
Figure 11. Dependence of the rate constant for the formation of Zncyt on GuHCl concentration at 25°C.

Incorporation of Zinc into H$_2$cyt as a Function of Urea. The complete incorporation of Zn^{2+} into H$_2$cyt forming Zncyt is confirmed by the shift in Soret absorbance band from 404 nm (characteristic of H$_2$cyt) to 423 nm (characteristic of Zncyt) and also the change in the region of 500 to 650 nm from four absorbance maxima to two. Specifically the decrease in absorbance at 506 nm is indicative of complete incorporation of Zn^{2+} into H$_2$cyt. The absorbance maxima in Zncyt are 423 nm, 540 nm and 580 nm.

Incorporation of Zn^{+2} in the H$_2$cyt was studied at different concentrations (1.0 M – 8.0 M) of urea. At lower concentrations (1.0 M), the incorporation was a slow process with a very gradual red shift in the Soret absorbance band over time. Two distinct Soret bands were observed after about 60 minutes, indicating a mixture of H$_2$cyt and Zncyt. At the end of the experiments, complete incorporation of Zn^{2+} was observed (**Figure 12**). At intermediate concentrations (5.0 M), the incorporation was very fast, with an immediate change in the Soret absorbance band, so that the conversion from H$_2$cyt to Zncyt could not be observed in the short time from placing the cuvette in the sample chamber and starting the collection of spectra (**Figure 13**). However, at higher concentrations (7.0 M), the incorporation was again slower with a gradual change in the Soret absorbance peak indicating that intermediate concentrations are more favorable for incorporation of Zn^{+2} into H$_2$cyt (**Figure 14**). Isobestic points again indicate that the conversion of H$_2$cyt into Zncyt takes place without the formation of any observable spectroscopic intermediates.

Figure 12. Zinc incorporation at low concentrations of urea. Absorbance spectra collected over time upon incorporation of Zn^{2+} into 7.5 µM H_2cyt in the presence of 1.0 M urea at 25°C. The concentration of Zn^{2+} is 100 µM. 20 spectra are collected at a time interval of 15 minutes for a total of 285 minutes.
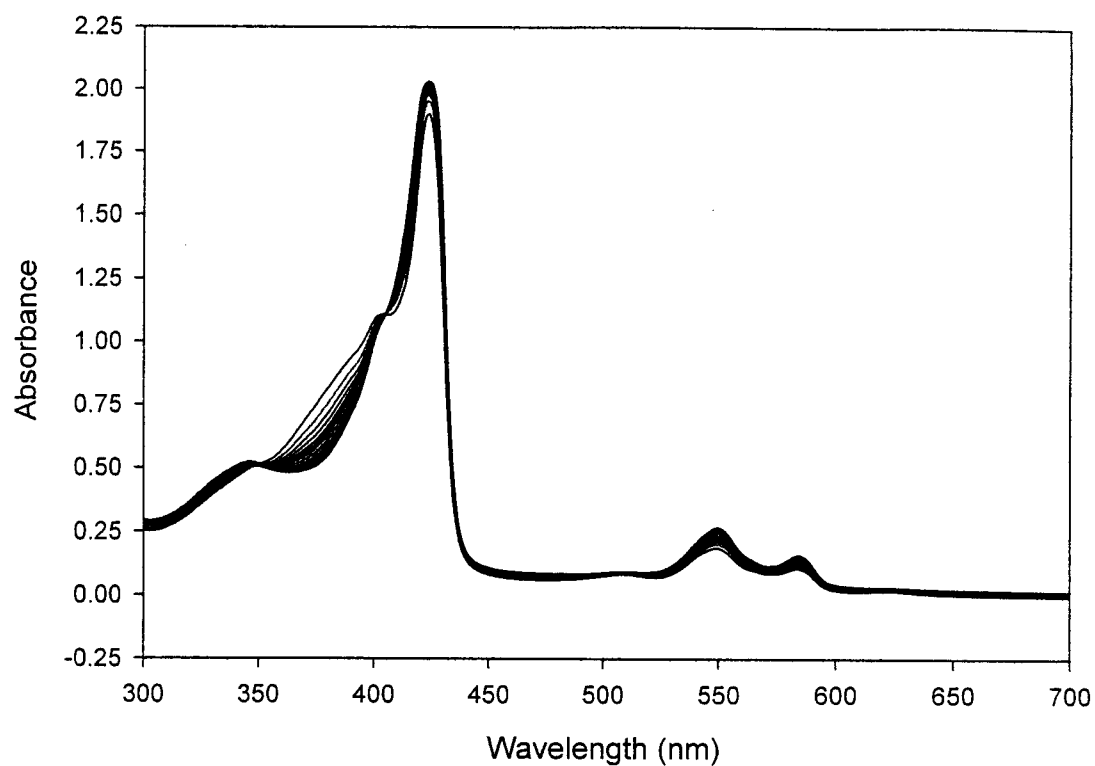
Figure 13. Zinc incorporation at intermediate concentrations of urea. Absorbance spectra collected over time upon incorporation of Zn^{2+} into 7.5 μM H_2cyt in the presence of 5.0 M urea at 25°C. The concentration of Zn^{2+} is 100 μM. 20 spectra are collected at a time interval of 5 minutes for a total of 95 minutes.
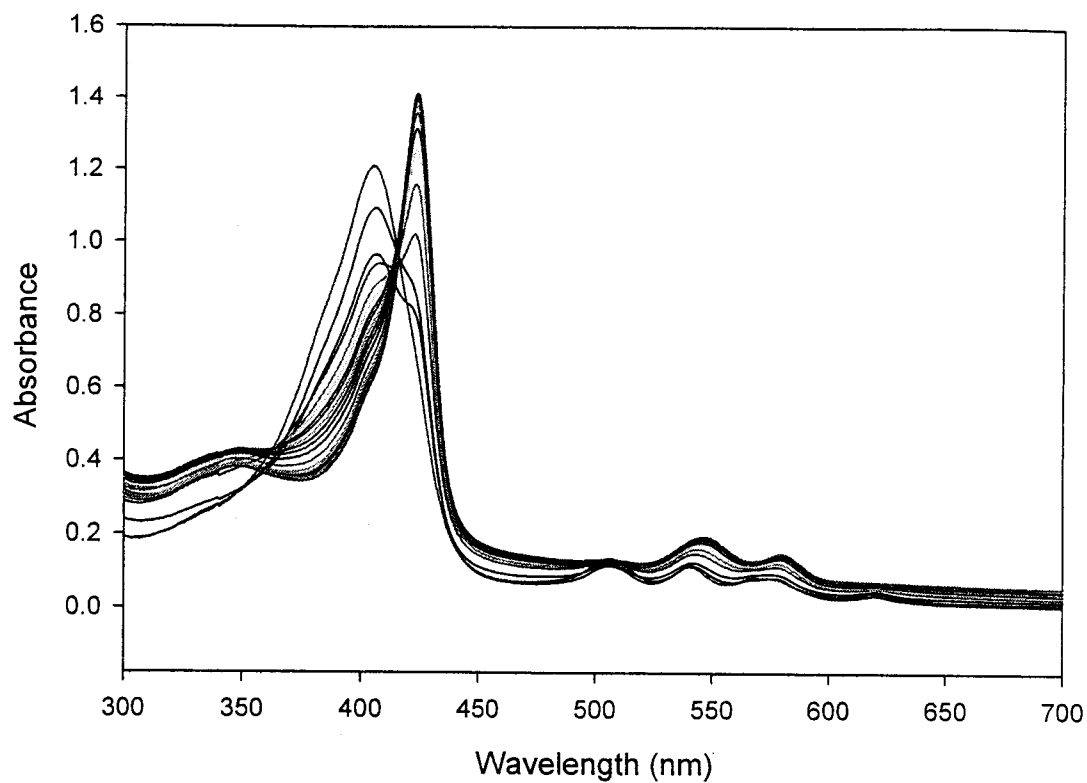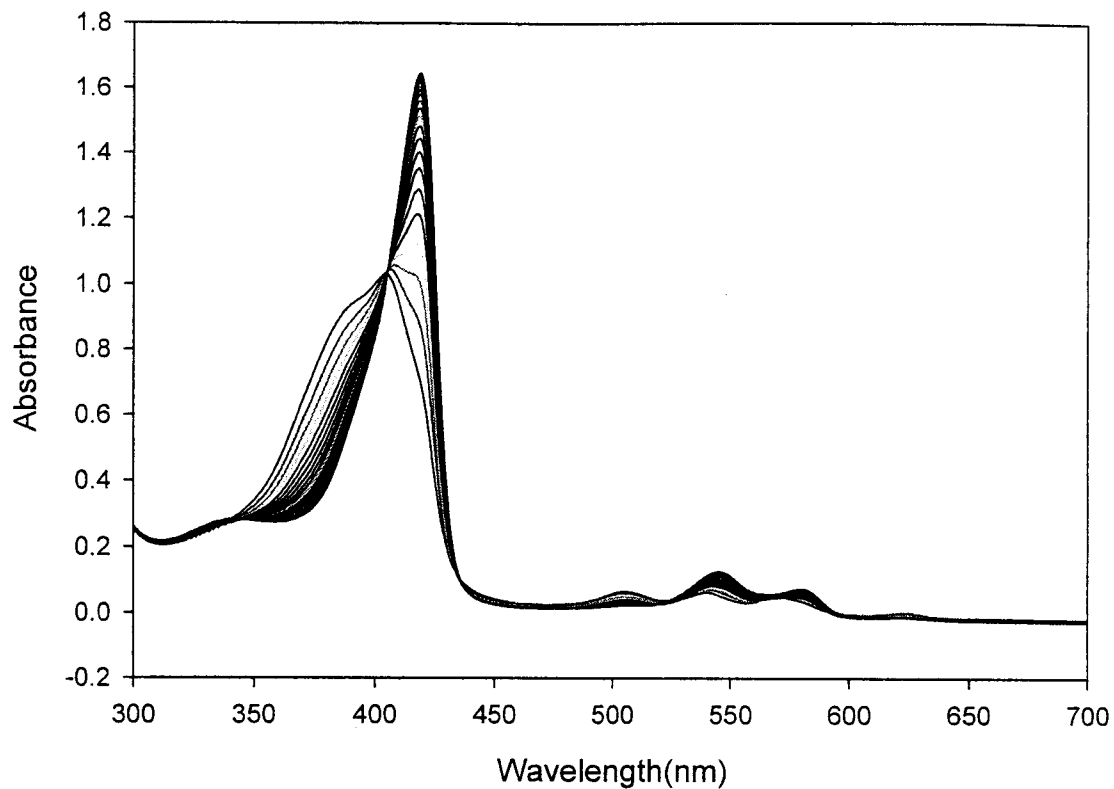
Figure 14. Zinc incorporation at high concentrations of urea. Absorbance spectra collected over time upon incorporation of Zn^{2+} into 7.5 μM H_2cyt in the presence of 7.0 M urea at 25°C. The concentration of Zn^{2+} is 100 μM. 20 spectra are collected at a time interval of 3 minutes for a total of 57 minutes.

Rate constants for the incorporations of Zn^{2+} in the H_2cyt were obtained from the changes in the absorbance at 404 nm and 423 nm. At lower concentrations of urea (1.0 M) where the incorporation was slow, the plots show a gradual exponential decay at 404 nm and gradual exponential rise at 423 nm (**Figure 15**). It takes about 120 minutes for complete incorporation. At intermediate concentrations of urea (5.0 M) incorporation was very fast. It takes about 20 minutes, only a few data points can be fitted to obtain the rate constants (**Figure 16**). There is virtually no change in absorbance at 404 nm, since the first collected absorbance spectrum is already that of $Zncyt$. At higher concentrations (7.0 M) the incorporation took almost 57 minutes, more than for the incorporation at intermediate concentrations and only a few data points can be fitted to obtain rate constants (**Figure 17**). Even at this concentration there is virtually no change in absorbance at 404 nm, since the first collected absorbance spectrum is already that of $Zncyt$. Overall, the rate constants obtained indicate the most rapid incorporation of Zn^{+2} into H_2cyt at intermediate concentrations urea. The rate constant at the intermediate (5.0 M) concentration of urea ($k_f = 0.077 \pm 0.011$ min^{-1}) is two times faster than the rate constant at low (1.0 M) concentration of urea ($k_f = 0.03200 \pm 0.00090$ min^{-1}) and is 1.5 times faster than at high (7.0 M) concentrations of urea ($k_f = 0.05100 \pm 0.00048$ min^{-1}).
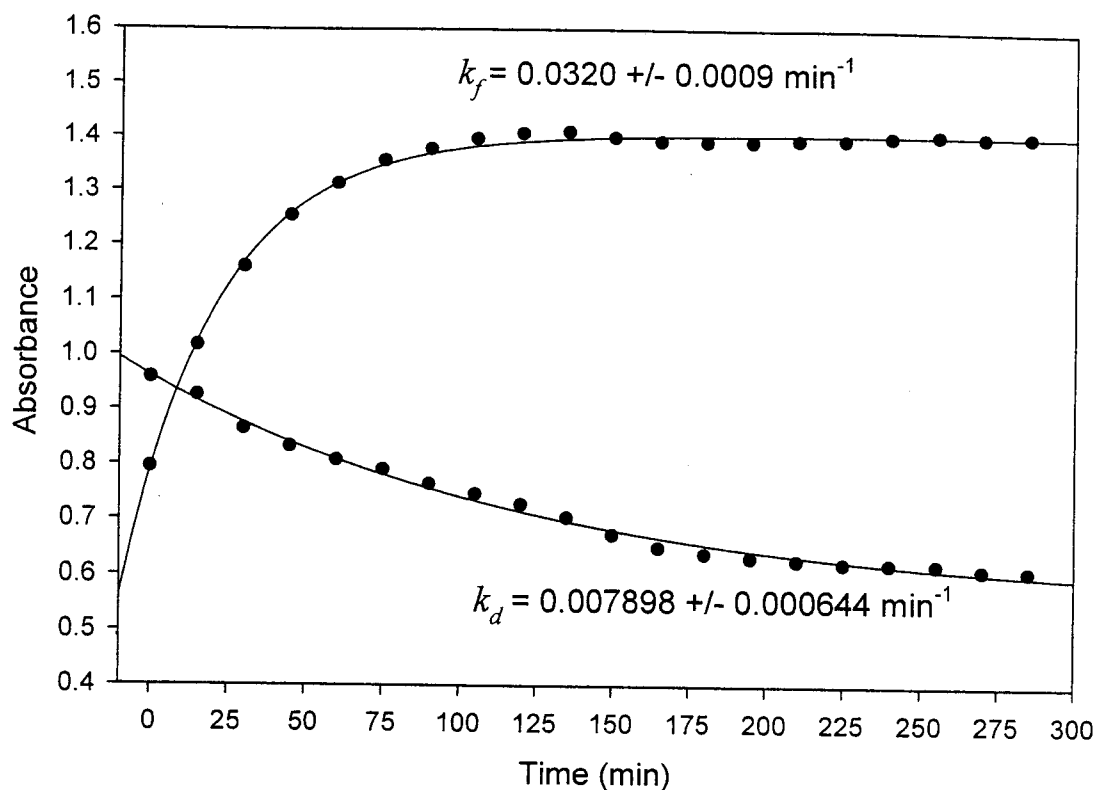
Figure 15. Rate Constant Plots for Zinc incorporation at low concentrations of urea. Change in heme Soret absorbance over time as Zn^{2+} is incorporated into H_2cyt in the presence of 1.0 M urea. Data points for the exponential decay at 404 nm and the exponential rise at 423 nm were plotted. Rate constants were obtained by fitting the data to monoexponential equations (equations 3 & 4 in the Materials and Methods Section) using SigmaPlot 8.0. Experimental conditions: 7.5 μM H_2cyt, 25°C, 100 μM Zn^{2+}. The error reported for rate constants k_d and k_f are the standard deviation for the fitting.
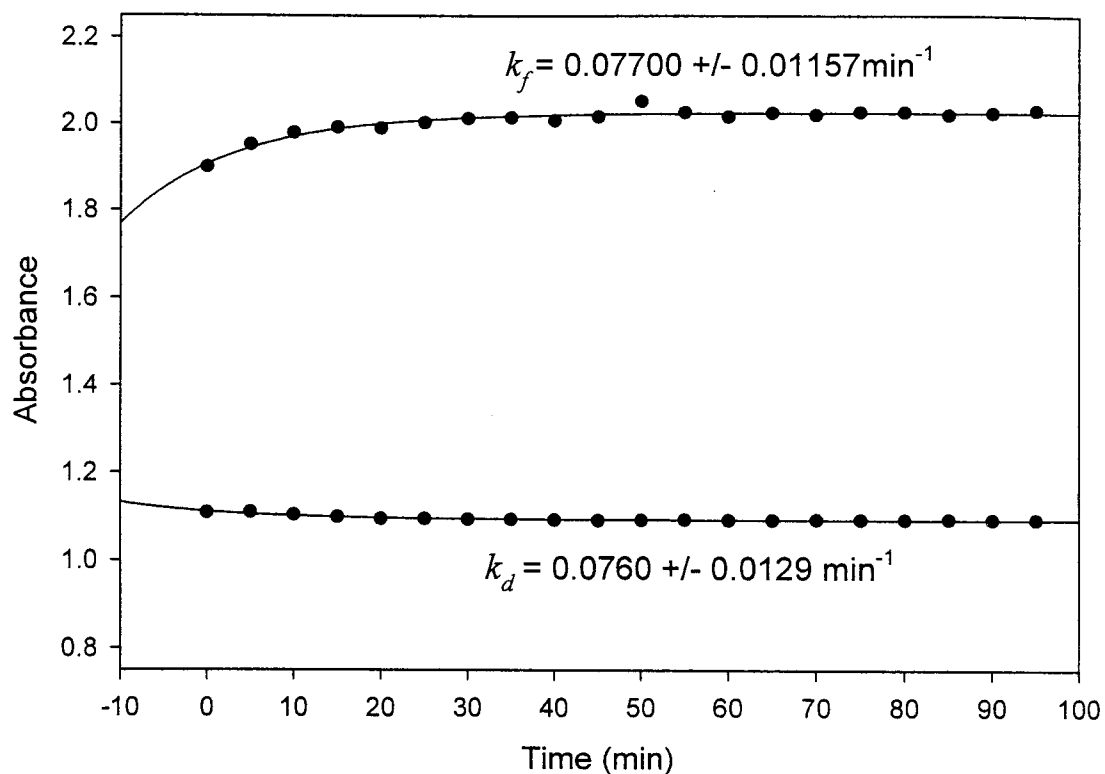
Figure 16. Rate Constant Plots for Zinc incorporation at intermediate concentrations of urea. Change in heme Soret absorbance over time as Zn^{2+} is incorporated into H_2cyt in the presence of 5.0 M urea. Data points for the exponential decay at 404 nm and the exponential rise at 423 nm were plotted. Rate constants were obtained by fitting the data to monoexponential equations (equations 3 & 4 in the Materials and Methods Section) using SigmaPlot 8.0. Experimental conditions: 7.5 μM H_2cyt, 25°C, 100 μM Zn^{2+}. The error reported for rate constants k_d and k_f are the standard deviation for the fitting.
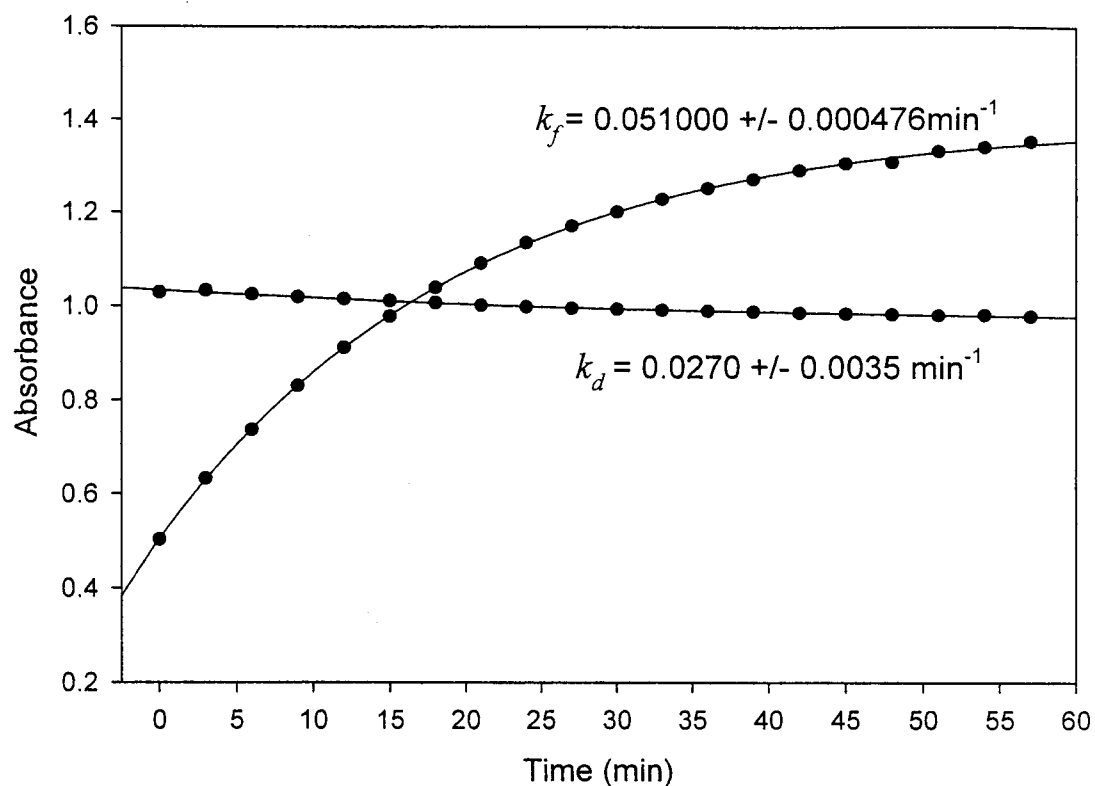
Figure 17. Zinc incorporation at high concentrations of urea. Change in heme Soret absorbance over time as Zn^{2+} is incorporated into H_2cyt in the presence of 7.0 M urea. Data points for the exponential decay at 404 nm and the exponential rise at 423 nm were plotted. Rate constants were obtained by fitting the data to monoexponential equations (equations 3 & 4 in the Materials and Methods Section) using SigmaPlot 8.0. Experimental conditions: 7.5 μM H_2cyt, 25°C, 100 μM Zn^{2+}. The error reported for rate constants k_d and k_f are the standard deviation for the fitting.

Incorporation of Copper into H$_2$cyt as a Function of Temperature. The complete incorporation of Cu^{2+} into H$_2$cyt forming Cucyt is shown by the shift in Soret absorbance band from 404 nm (characteristic of H$_2$cyt) to 422 nm (characteristic of Cucyt) and also the change in the region of 500 to 650 nm from four absorbance maxima to two. Specifically, the decrease in absorbance at 506 nm is indicative of complete incorporation of Cu^{2+} into H$_2$cyt. The absorbance maxima in Cucyt are 422 nm, 540 nm and 580 nm.

Incorporation of Cu^{+2} into H$_2$cyt was studied at different temperatures (40°C – 55°C). At lower temperatures (40°C), the incorporation was a slow process with a very gradual shift in the Soret absorbance band over time, leading to the presence of two distinct Soret bands indicating two spectroscopic forms of Cucyt (**Figure 18**). At intermediate temperatures (45°C and 50°C), the incorporation was fast, although the first collected spectrum after 5 minutes still shows a distinct absorbance peak at 506 nm indicating the presence of H$_2$cyt (**Figures 19 and 20**). At the highest temperature (55°C) incorporation was very fast, with a virtually immediate change in the Soret absorbance band, so that the conversion from H$_2$cyt to Cucyt could not be observed in the short time from placing the cuvette in the sample chamber and starting the collection of spectra (**Figure 21**). Throughout the experiment, only one peak is observed at 422 nm indicating the presence of Cucyt.

Rate constants for the incorporation were obtained from the changes in the absorbance at 404 nm and 422 nm. At lower temperatures (40°C), incorporation was a slow process, so the rate constant was also small (0.090±0.212 min^{-1}). In this case, the rate constant for the decay of H$_2$cyt(0.090±0.212 min^{-1}) and the formation of Cucyt

(0.0910±0.0158 min^{-1}) are similar indicating that a single process is taking place. Incorporations at higher temperatures (45°C, 50°C and 55°C) are very fast, only few points can be obtained to fit the rate constants. It actually reaches the rate constant limit of our instrument when collecting respective spectra every three minutes (0.3 min^{-1}). To study such rapid metal ion incorporation experiments, much smaller time intervals between spectra should be chosen, or else follow the change in absorbance at only one or two wavelengths as this allows time intervals in the sub second range.

Figure 18. Copper incorporation at low temperatures (40°C). Absorbance spectra collected over time upon incorporation of Cu^{2+} into 7.5 µM H$_2$cyt at 40°C. The concentration of Cu^{2+} is 100 µM. 20 spectra are collected at a time interval of 15 minutes for a total of 285 minutes.

Figure 19. Copper incorporation at intermediate temperatures (45°C). Absorbance spectra collected over time upon incorporation of Cu^{2+} into 7.5 μM H_2cyt at 45°C. The concentration of Cu^{2+} is 100 μM. 20 spectra are collected at a time interval of 5 minutes for a total of 95 minutes.

Figure 20. Copper incorporation at intermediate temperatures (50°C). Absorbance spectra collected over time upon incorporation of Cu^{2+} into 7.5 µM H_2cyt at 50°C. The concentration of Cu^{2+} is 100 µM. 20 spectra are collected at a time interval of 3 minutes for a total of 57 minutes.
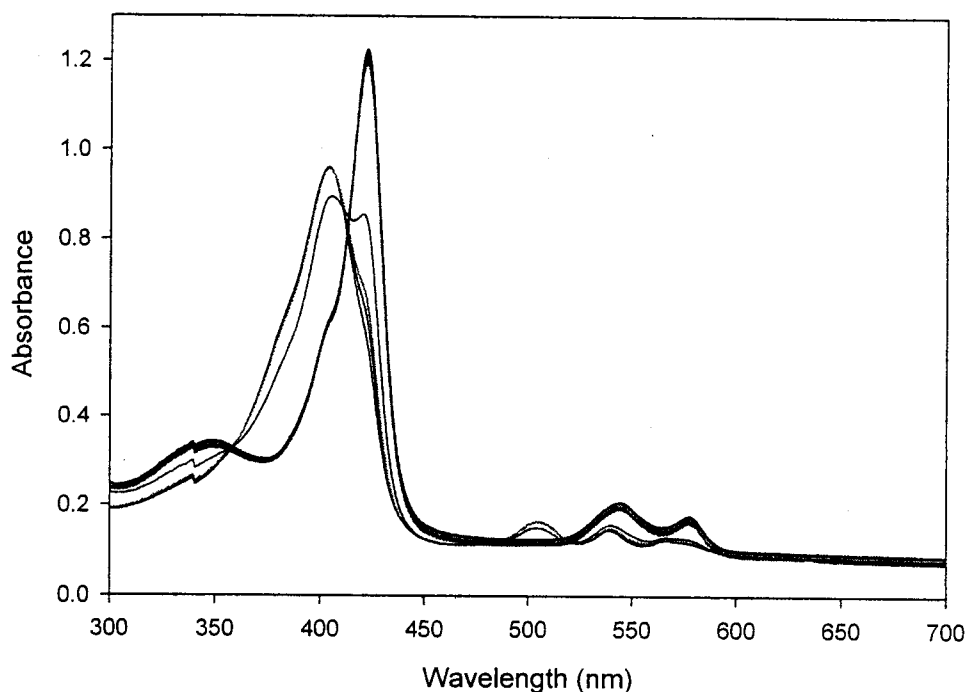
Figure 21. Copper incorporation at high temperatures (55°C). Absorbance spectra collected over time upon incorporation of Cu^{2+} into 7.5 μM H_2cyt at 55°C. The concentration of Cu^{2+} is 100 μM. 20 spectra are collected at a time interval of 2 minutes for a total of 38 minutes.

Incorporation of Copper into H₂cyt as a Function of GuHCl. The complete

incorporation of Cu^{2+} into H_2cyt forming Cucyt is shown by the shift in Soret absorbance

band from 404 nm (characteristic of H_2cyt) to 390 nm, 403 nm and 422 nm (characteristic

of different forms of Cucyt) and also the change in the region of 500 to 650 nm from four

absorbance maxima to two. Specifically, the decrease in absorbance at 506 nm is

indicative of complete incorporation of Cu^{2+} into H_2cyt. The absorbance maxima in all

three forms of Cucyt are 390, 403, or 422 nm, 540 nm and 580 nm.

Incorporation of Cu^{+2} in the H_2cyt was studied at different concentrations of

GuHCl (0.5 M – 4 M). At lower concentrations (0.5 M), the incorporation was a slow

process with a very gradual shift in the Soret absorbance band over time, from 404 nm to

422 nm with a small shoulder at 403 nm indicating the presence of two forms of Cucyt

(**Figure 22**). At another low concentration (1.0 M), the incorporation took place with a

gradual shift in the peak from 404 nm to maxima peak at 403 nm, small peak at 422 nm

and a small shoulder at 390 nm indicating the formation of three forms of Cucyt (**Figure

23**). At intermediate concentrations (1.5 M and 2.0 M), incorporation was very fast, with

presence of two peaks at 390 nm and 403 nm indicating two forms of Cucyt. At higher

concentrations (2.5 M – 4.0 M), the incorporation was very fast, with a virtually

immediate change in the Soret absorbance band from 404 nm to 390 nm, indicating the

formation of only one form of Cucyt (**Figure 24**). These indicate the formation of

different spectral forms of Cucyt with change in the concentration of GuHCl. These

experiments were repeated twice with same results.
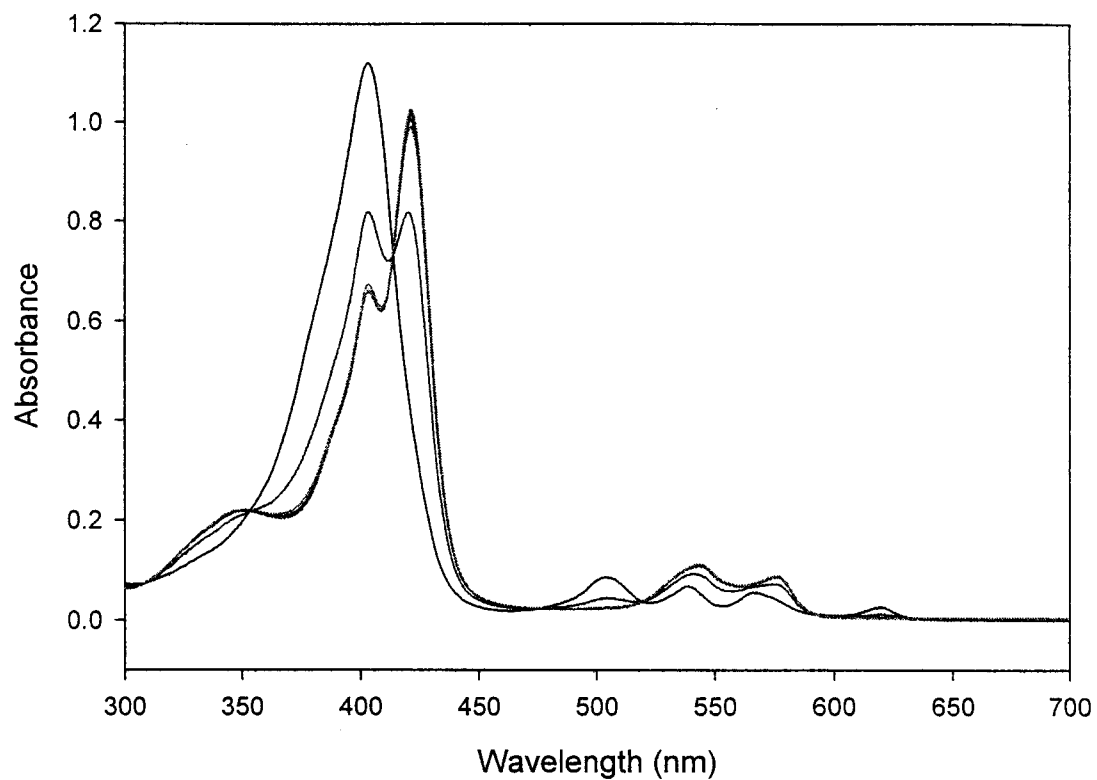
Figure 22. Copper incorporation at low concentrations of GuHCl. Absorbance spectra collected over time upon incorporation of Cu^{2+} into 7.5 µM H_2cyt in the presence of 0.5 M GuHCl at 25°C. The concentration of Cu^{2+} is 100 µM. 20 spectra are collected at a time interval of 15 minutes for a total of 285 minutes.
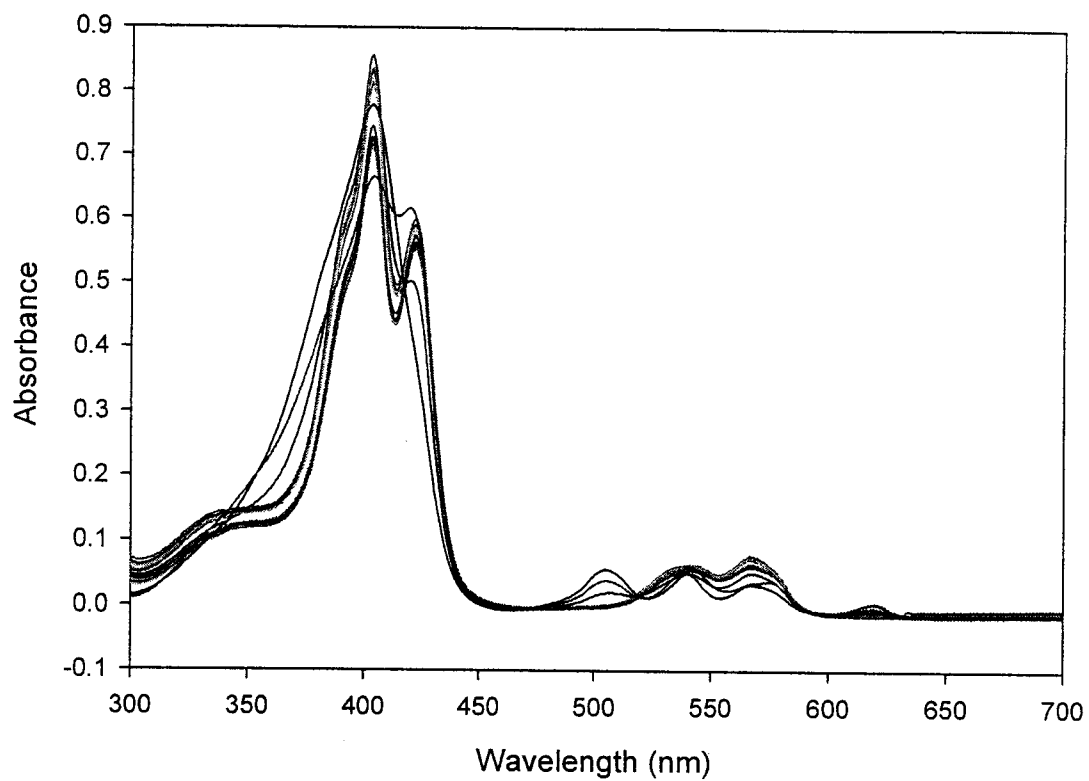
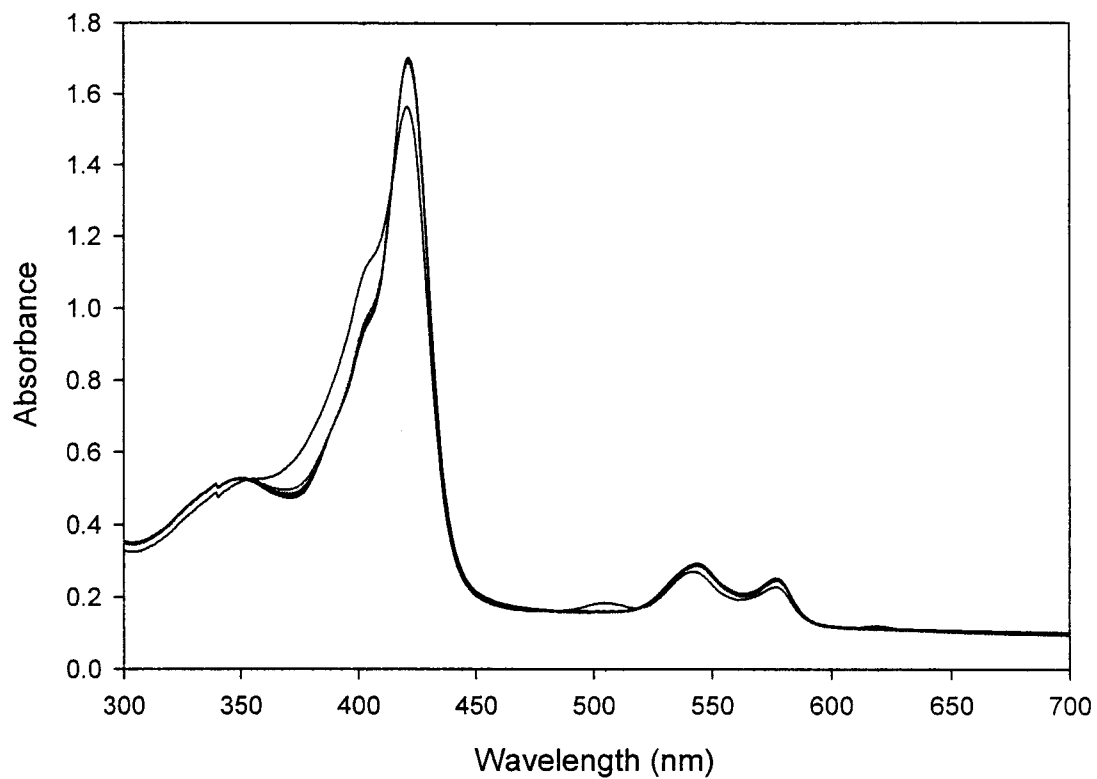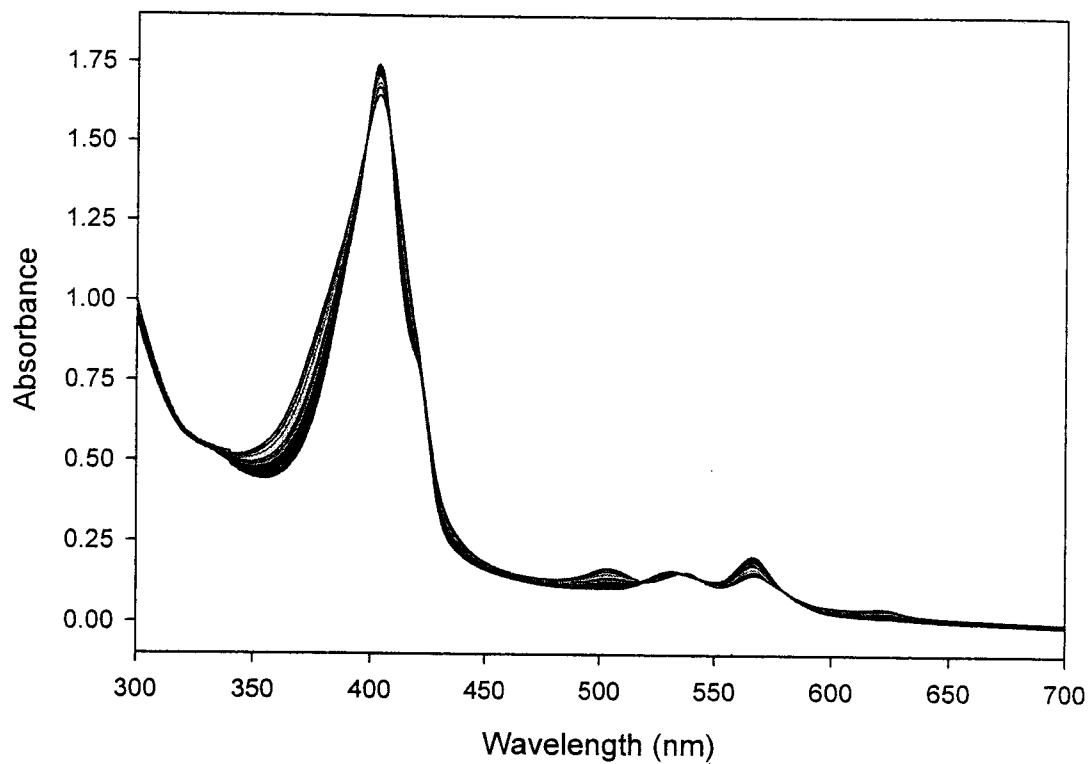**Figure 23. Copper incorporation at intermediate concentrations of GuHCl.**
Absorbance spectra collected over time upon incorporation of Cu^{2+} into 7.5 µM H_2cyt in the presence of 1.0 M GuHCl at 25°C. The concentration of Cu^{2+} is 100 µM. 20 spectra are collected at a time interval of 10 minutes for a total of 190 minutes.

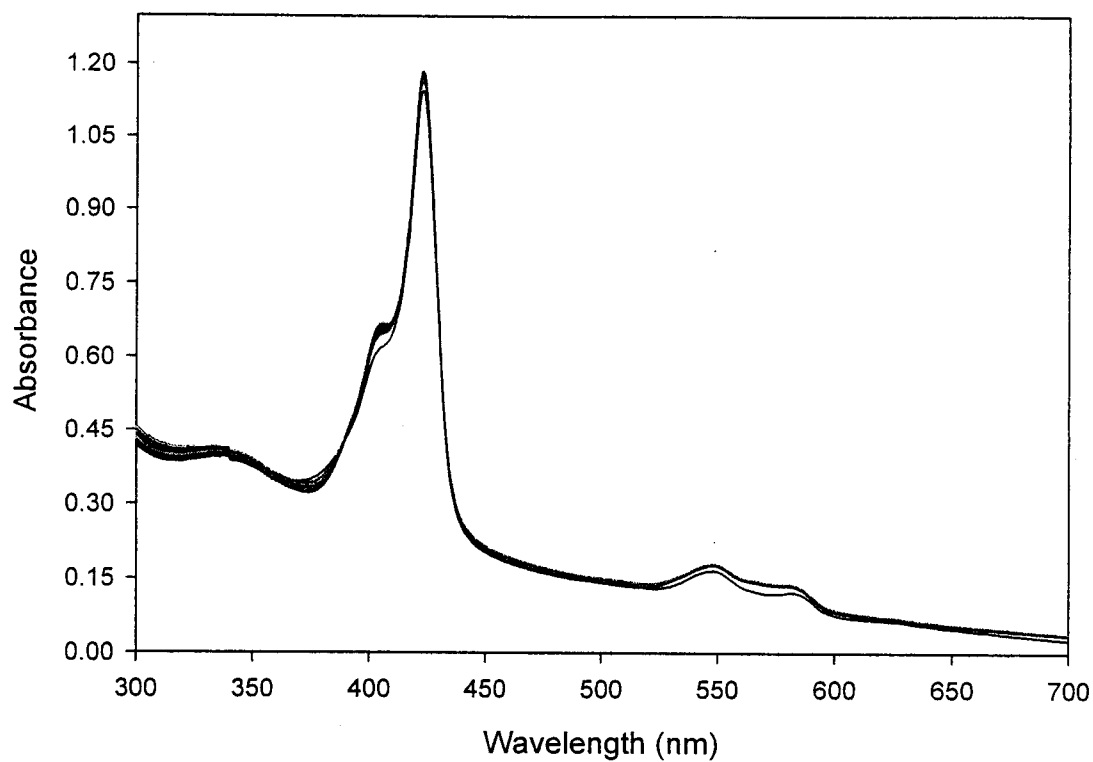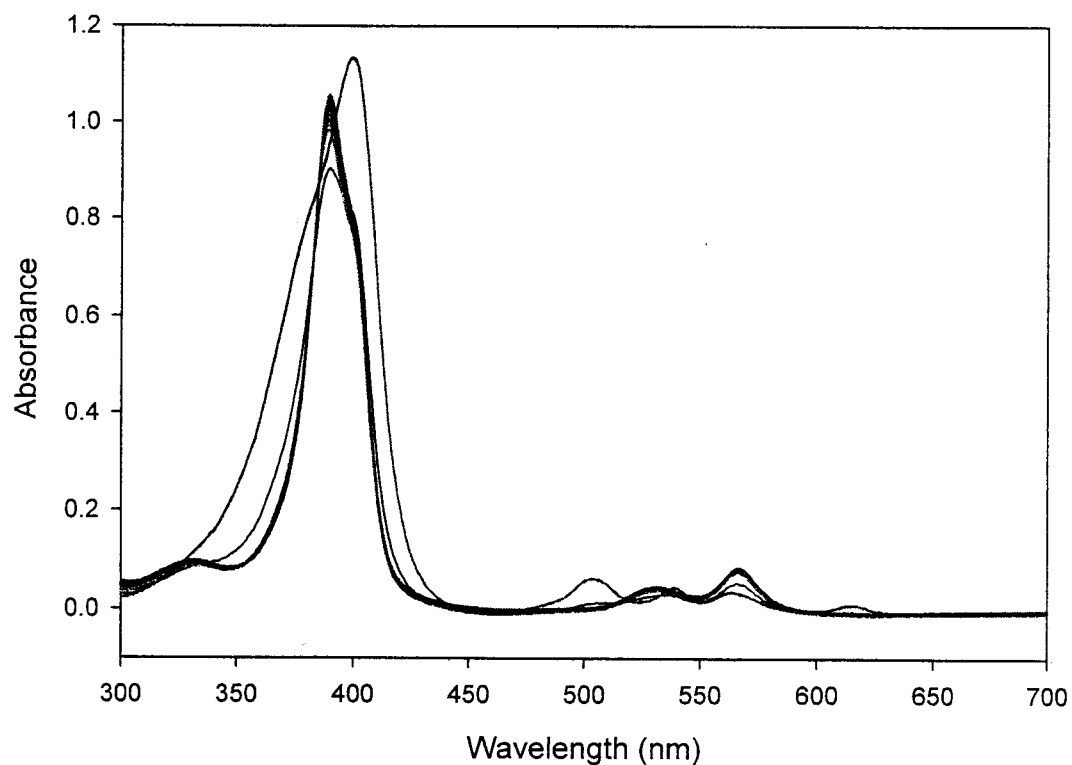**Figure 24. Copper incorporation at high concentrations of GuHCl.** Absorbance spectra collected over time upon incorporation of Cu^{2+} into 7.5 μM H_2cyt in the presence of 3.0 M GuHCl at 25°C. The concentration of Cu^{2+} is 100 μM. 20 spectra are collected at a time interval of 5 minutes for a total of 95 minutes.

The three different spectroscopic forms of Cucyt obtained depended on the concentration of GuHCl (0.5 M – 4.0 M). These forms show Soret absorbance maxima at 390 nm, 403 nm and 422 nm (**Figure 25** and **Table I**).
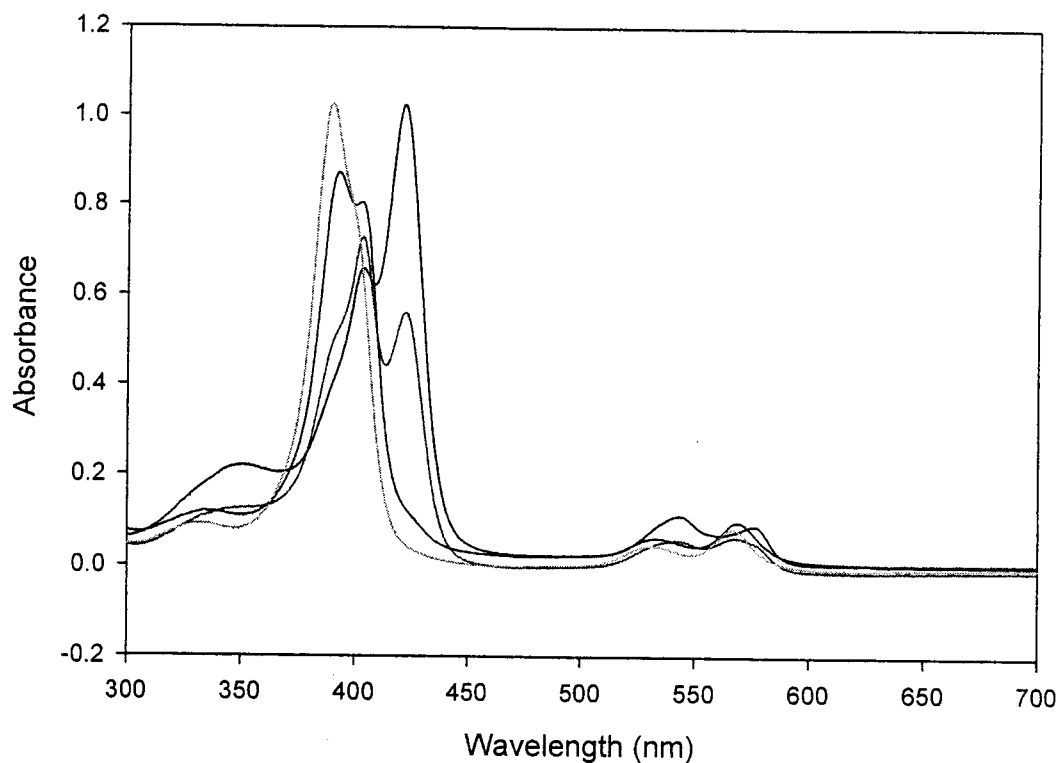
Figure 25. Conformational forms of Cucyt at different concentrations of GuHCl.
Different forms of Cucyt obtained upon incorporation of Cu^{2+} into 7.5 μM H_2cyt in the presence of different concentrations of GuHCl (0.5 M – 4 M) at 25°C. Spectra clearly show different forms of Cucyt in different concentrations of GuHCl. The concentration of Cu^{2+} is 100 μM.

Table I. Soret absorbance maxima of different conformational forms of Cucyt in various concentrations of GuHCl

[GuHCl] (M)	Soret Absorbance Maxima (nm)		α/β Band Absorbance Maxima (nm)	
0.5	403.4	422	543.2	575
1.0	403	420	540.4	567.4
3.0	390		538	565.5

Equilibrium Unfolding of Cucyt Monitored by Tryptophan Fluorescence.

Tryptophan florescence emission spectra provide information on the unfolding of Cucyt.

The complete unfolding of Cucyt was confirmed by the shift of the fluorescence intensity

peak at 331 nm at low concentrations of GuHCl (0.25 M) to 350 nm at high concentration

of GuHCl (4.0 M). As the concentration of GuHCl increases from 0.25 M to 4.0 M, the

fluorescence emission intensity decreases (**Figure 26**).
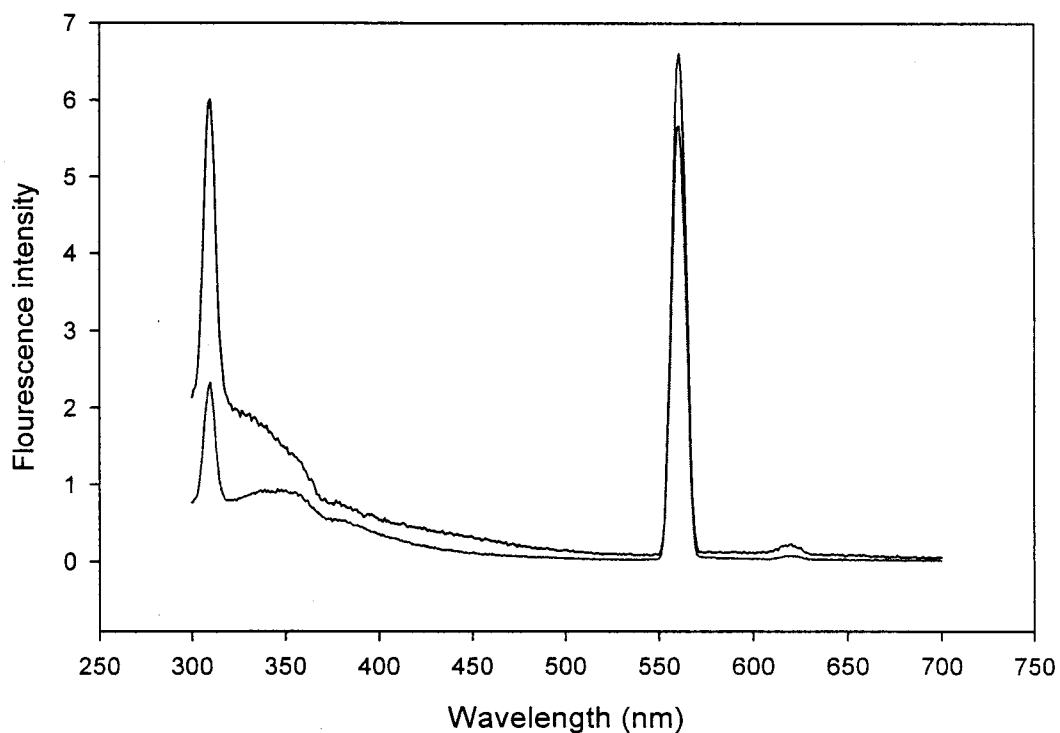
Figure 26. Fluorescence emission spectra of Cucyt in GuHCl. Fluorescence emission spectra of Cucyt collected after 4 hours in the presence of 0.25 M and 4.0M GuHCl at 25°C. The concentration of Cucyt is 0.1 μM. Nine spectra are collected for each concentration at time intervals of 30 minutes for a total of 4 hours.

Cucyt structural stability was determined by measuring the tryptophan

fluorescence emission over a range of GuHCl concentrations. The fraction of unfolded

Cucyt at different concentrations of GuHCl (0.25 M – 4.25 M) was obtained. With an

increase in concentration of GuHCl, the amount of Cucyt unfolding increases. The

midpoint for the unfolding transition (C_m) is 2.61±0.24 M (**Figure 27a**). The experiment

was repeated under the same conditions and C_m = 2.79±0.54 M (**Figure 27b**).
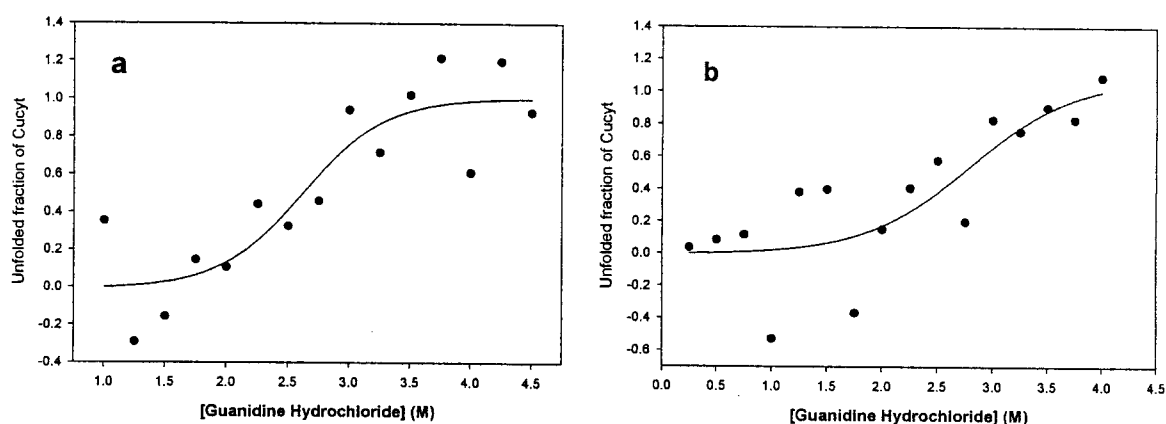
Figure 27. Equilibrium unfolding of Cucyt at different concentrations of GuHCl.
(a) Equlibrium unfolding of 0.1 μM Cucyt at 25°C induced by 0.5 M – 4.5 M GuHCl and
monitored by tryptophan fluorescence emission at 331 nm. The data are fitted to a four
parameter sigmoidal equation with the midpoint for the unfolding transition (C_m) at
2.61±0.24 M. (b) Repetition of the experiment under the same conditions with the
midpoint for the unfolding transition (C_m) at 2.79±0.54 M.

To obtain the free energy for the unfolding of Cucyt in the absence of denaturant (ΔG_U), linear regression is used to extrapolate the experimental values for ΔG_U in the region of 1.5 M to 3.5 M GuHCl. For Cucyt, ΔG_U is 19.4±5.5 kJ/mol (**Figure 28a**). The experiment was repeated under the same conditions and ΔG_U = 14.8±4.7 kJ/mol (**Figure 28b**).
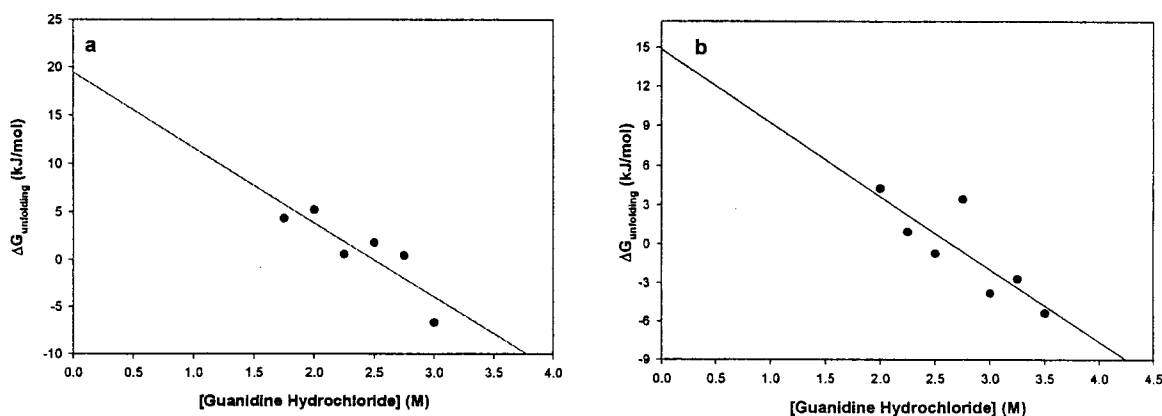
Figure 28. Plot of the free energy for unfolding Cucyt as a function of GuHCl concentration. (a) Equilibrium unfolding of 0.1 μM Cucyt at 25°C induced by 0.5 M – 4.5 M GuHCl and monitored by tryptophan fluorescence at 331 nm. The free energy for unfolding (ΔG_U) values are calculated using the equation 5 (Materials and Methods section). ΔG_U is 19.4±5.5 kJ/mol. (b) Repetition of the experiment under the same conditions with ΔG_U = 14.8±4.7 kJ/mol.

Cucyt structural stability was determined by measuring the tryptophan fluorescence emission over a range of urea concentrations. The fraction of unfolded Cucyt at different concentrations of urea (3.75 M – 7.25 M) was obtained. With an increase in concentration of urea, the amount of Cucyt unfolding increases. The midpoint for the unfolding transition (C_m) is 4.74 M (**Figure 29a**). The experiment was repeated under the same conditions and C_m = 5.58 M (**Figure 29b**).
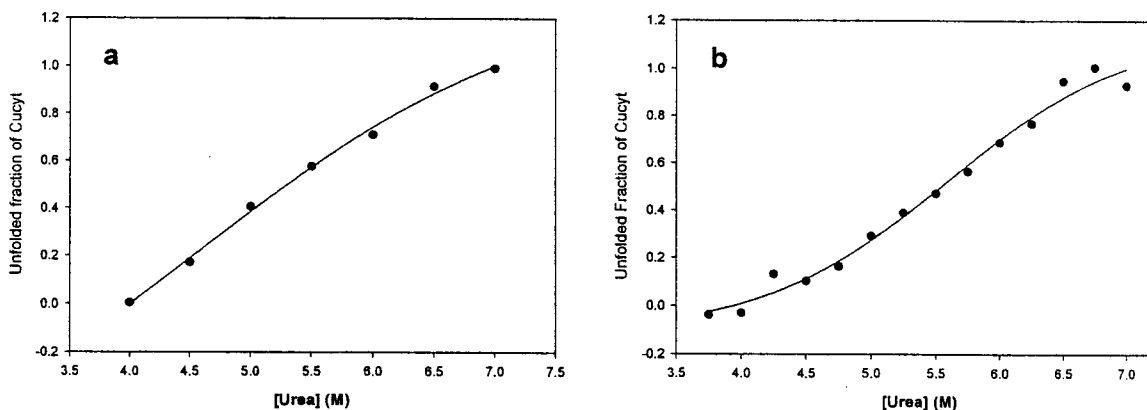
Figure 29. Equilibrium unfolding of Cucyt at different concentrations of urea. (a) Equilibrium unfolding of 0.1 μM Cucyt at 25°C induced by 3.75 M – 7.25 M urea and monitored by tryptophan fluorescence emission at 331 nm. The data are fitted to a four parameter sigmoidal equation with the midpoint for unfolding transition (C_m) at 4.74 M. (b) Repetition of the experiment under the same conditions with the midpoint for the unfolding transition (C_m) at 5.58 M

To obtain the free energy for the unfolding of Cucyt in the absence of denaturant

(ΔG_U), linear regression is used to extrapolate the experimental values for ΔG_U in the

region of 4.50 M to 6.50 M urea. For Cucyt, ΔG_U is 23.8±2.3 kJ/mol (**Figure 30a**). The

experiment is repeated under the same conditions and ΔG_U is 25.5±1.1 kJ/mol (**Figure**

30b).
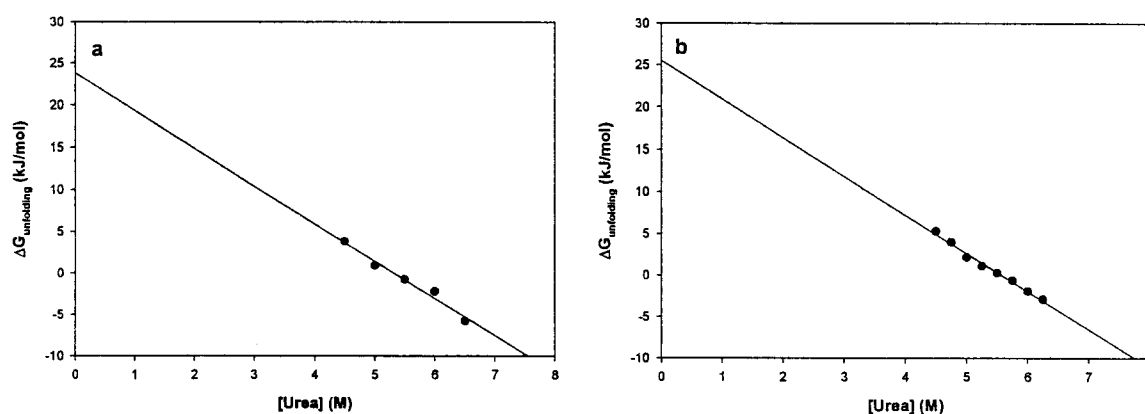
Figure 30. Plot of the free energy for unfolding Cucyt as a function of urea concentration. (a) Equlibrium unfolding of 0.1 µM Cucyt at 25°C induced by 3.75 M – 7.25 M urea and monitored by tryptophan fluorescence emission at 331 nm. The values for free energy for unfolding (ΔG_U) are calculated using the equation 5 (Materials and Methods section). ΔG_U is 23.8±2.3 kJ/mol. (b) Repetition of the experiment the under same conditions with ΔG_U = 25.5±1.1 kJ/mol.

In temperature-induced unfolding experiments on Cucyt, it was observed that an increase in the temperature causes a decrease in the tryptophan fluorescence emission intensity. Therefore, as the temperature of Cucyt in the cuvette increases from 15°C – 90°C, there is steady decrease in the emission intensity (**Figure 31**).
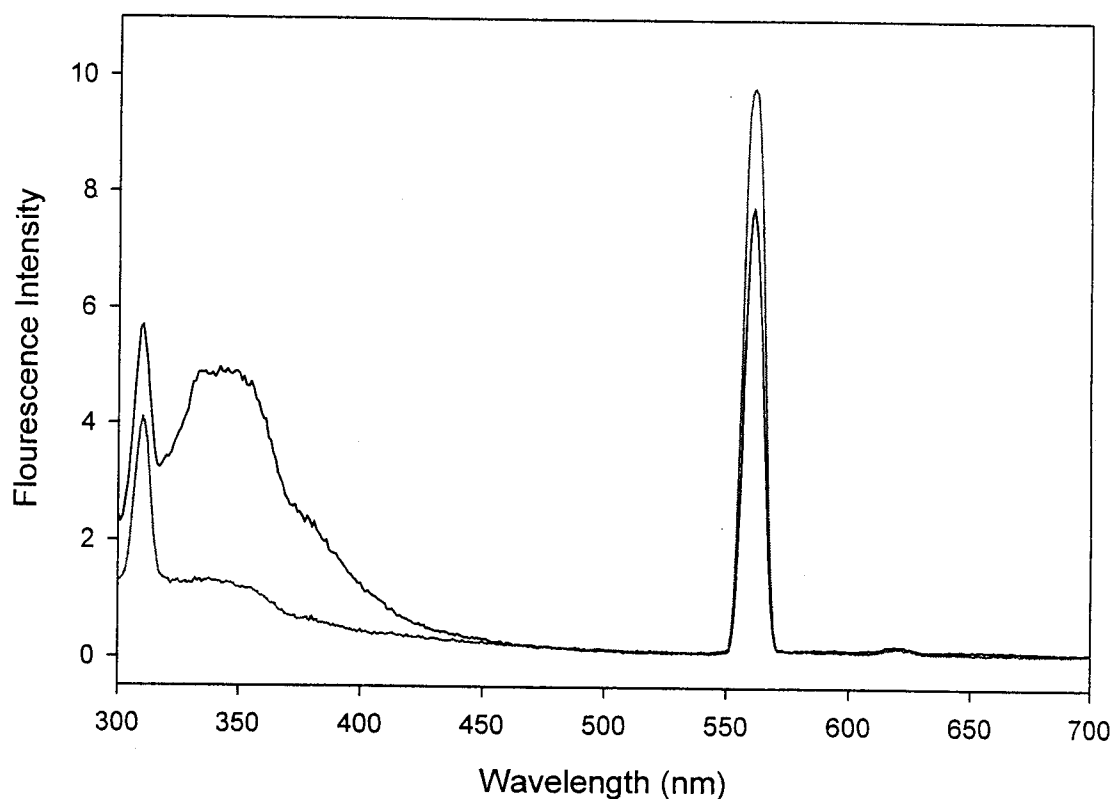
Figure 31. Florescence emission spectra of Cucyt in water at different temperatures. Fluorescence emission spectra of Cucyt collected at 15°C (top) and 90°C (bottom). The concentration of Cucyt is 0.1 µM.

CHAPTER 4.

DISCUSSION

Metal Ion Contamination in Porphyrin Cytochrome *c* Monitored by Heme Soret Absorbance. One problem encountered in these metal ion incorporation experiments is the presence of contaminating metal ions in preparations of H_2cyt. Nearly all preparations of purified H_2cyt have never exhibited this problem, however, one recently prepared batch did. This contamination interferes and/or competes with the incorporation of the desired metal ion (Zn^{2+} or Cu^{2+}). In this study, H_2cyt is dissolved in a solution of GuHCl at various concentrations and the change in the heme Soret absorbance is monitored over time. The H_2cyt and metal substituted cytochrome *c* have significantly different heme Soret absorbance spectra. GuHCl is a strongly alkaline, water-soluble compound that efficiently unfolds proteins by perturbing protein:protein, protein:solvent, and solvent:solvent interactions, such as electrostatic interactions and hydrogen bonds. In the folded state, H_2cyt has a compact structure with porphyrin buried in the hydrophobic core. In the presence GuHCl, it unfolds and facilitates the incorporation of a metal ion into the porphyrin forming metal substituted cytochrome *c*. At every GuHCl concentration except the very lowest (0.0001 M), the results in **Figures 2 – 4** clearly indicate incorporation of a contaminating metal ion. The heme Soret absorbance band shifts from 404 nm to 423 nm and the four peaks in the region of 500 to 600 nm, characteristic of H_2cyt, are converted into only 2 peaks, characteristic of metal substituted cytochrome *c*). Therefore, this preparation of H_2cyt has a metal ion impurity. The incorporation of contaminating metal ion in H_2cyt was also found to be dependent on

the concentration of GuHCl. At lower concentrations of GuHCl, partial incorporation of a contaminating metal ion is observed. Under these conditions, H_2cyt is only partially unfolded with the porphyrin only partially exposed to solvent. At higher concentrations of GuHCl, complete incorporation of a contaminating metal ion is observed. Under these conditions, H_2cyt is completely unfolded with the porphyrin completely exposed to solvent.

Another goal of these experiments was to determine the lowest concentration of GuHCl that does not bring about any protein conformational changes. Metal ion incorporation can be a sensitive probe of tertiary structure and porphyrin accessibility. As the protein partially and completely unfolds with the expansion or opening up of the hydrophobic core, metal ion incorporation will occur. Previous studies on other proteins (horseradish peroxidase & prothrombin) have shown that even GuHCl concentrations as low as 0.1 M induce changes in tertiary structure while leaving the native secondary structure and biological activity intact.[50] Not only did we observe changes in the Soret absorbance and therefore incorporation of contaminating metal ions at 0.1 M (**Figure 2**), but also at 0.01 M and 0.001 M GuHCl (data not shown). At these low concentrations, partial metal ion incorporation is therefore a result of a slight disruption of the protein's tertiary structure with the increase in accessibility of the hydrophobic core and porphyrin prosthetic group. It was not until very low concentrations of GuHCl (0.0001 M) that changes in the heme Soret absorbance were no longer observed (**Figure 1**). At this point, metal ion incorporation is prevented, indicating the protein's overall tertiary structure is intact and the hydrophobic core buried within the protein's interior. The porphyrin is no longer accessible to solvent and metal ion incorporation.

The change in the Soret absorbance over time is also an indicator of the protein's overall tertiary structure and porphyrin accessibility. At higher concentrations of GuHCl (2.5 M), metal ion incorporation was very fast, taking only 24 minutes for complete incorporation. The porphyrin is clearly accessible for metal ion incorporation. At intermediate concentrations of GuHCl (0.5 M), metal ion incorporation was slow, taking almost 285 minutes for complete incorporation. At lower concentrations of GuHCl (0.1 M), metal ion incorporation was slow, and in fact, only partial incorporation was observed after 285 minutes. This indicates the porphyrin is only partially accessible for metal ion incorporation. Finally at the lowest concentration of GuHCl (0.0001 M), no metal ion incorporation was observed, even after 1960 minutes, indicating the protein tertiary structure is intact and the porphyrin is buried in the hydrophobic core.

Possible sources of contamination in this preparation of H_2cyt may most likely be due to iron ions not removed from the H_2cyt solution via desalting after HF(g) addition to iron cytochrome c, impurities present in the denaturant (GuHCl) and metal salt, or quartz cuvettes contaminated with metal ions from previous experiments. Desalting separates large proteins from smaller ionic salts, so if this separation process fails, iron ions will be present in the purified H_2cyt. Iron ions are likely not the contaminating metal ion because the absorbance spectrum after contaminating metal-ion incorporation shows a sharp heme Soret absorbance at 423 nm, which is significantly red shifted to that of iron cytochrome c (**Figure 4**). To further confirm that iron is not the contaminating metal ion, potassium ferricyanide and ascorbic acid were added to the cuvette solution. These reagents readily cause oxidation and reduction of iron cytochrome c, resulting in

significant changes in the heme Soret absorbance spectrum. We observed no change in the absorbance spectrum, so iron is not a significant impurity (data not shown).

Since the concentrations of denaturant are typically very high (up to 4.0 M) in our experimental, GuHCl could be a possible source of the contaminating metal ion. The major impurities listed in GuHCl are Cu (<0.1 ppm), Fe (0.4 ppm), and heavy metals (2 ppm). The concentrations of impurities in the cuvette solutions used in our experiments are 0.6 μM Cu^{2+}, 2.7 μM Fe^{3+}, and 36.8 μM heavy metals (such as Pb^{2+}). The concentrations of Cu^{2+} and Fe^{3+} are less than the concentration of the H_2cyt (7.5 μM) used for the experiment. These low concentrations most likely will not interfere in the study of the incorporation of the desired metal ion (Zn^{2+} or Cu^{2+}) in H_2cyt, especially in the presence of 100 μM Zn^{2+} or Cu^{2+} that were used in our incorporation experiments. Although the concentration of heavy metals in the cuvette solution is five times greater than the concentration of H_2cyt, these metal ions have ionic radii too large to fit into the porphyrin. Therefore, it is unlikely that these heavy metals were responsible for the metal ion contamination observed.

Another possible source of contamination is the metal salt solutions themselves. We obtained high-purity metal ion salts (99.99% $CuCl_2$ and 99.99% $Zn(C_2H_3O_2)_2$) with impurities of 1 ppm iron and ~0.1 ppm each of other various metal ions. The concentrations of these impurities in the cuvette (for example, $[Fe^{3+}] = 2$ nM) will be significantly less than the concentration of H_2cyt or the desired metal ion (Cu^{2+} or Zn^{2+}). So contamination by these metal salts is negligible.

A likely candidate for the contaminating metal ion is Zn^{2+}. The heme Soret absorbance in Zncyt and this metal-contaminated cytochrome c are very similar, both

exhibiting a sharp peak at 423 nm. The likely source of Zn^{2+} contamination is from the quartz cuvettes that were previously used for the Zn^{2+} experiments. The cuvettes should be cleaned very well before and after each experiment. Hence, it is important to investigate whether or not contaminating metal ions are present and use proper laboratory technique, such as purchasing high purity reagents and acid washing all glassware, to limit the presence of contaminating metal ions. Although not directly studied in this thesis, metal ion incorporation experiments have been performed in the presence of EDTA to determine the concentration at which EDTA will prevent incorporation by contaminating metal ions, yet ensure complete incorporation of the metal ion of interest.

Incorporation of Zinc into H$_2$cyt as a Function of GuHCl. In this study, H$_2$cyt is dissolved in a solution of GuHCl at various concentrations and the change in the Soret absorbance is monitored over time. The goal is to determine the effect of GuHCl concentration on the rate of incorporation of Zn^{2+}. As the concentration of GuHCl increases, H$_2$cyt should unfold and allow faster incorporation of Zn^{2+} into the porphyrin. The H$_2$cyt and Zncyt have significantly different heme Soret absorbance spectra, facilitating the monitoring of H$_2$cyt decay and Zncyt formation over time. In our incorporation experiments, we clearly see the formation of Zncyt, indicated by the appearance of a peak at 423 nm (**Figures 5 – 7**). Moreover, the decrease in absorbance at 506 nm indicates complete incorporation of Zn^{2+} into H$_2$cyt (i.e., all H$_2$cyt has been converted into Zncyt). These observed absorbance spectra match those in the literature for Zncyt.[5]

The conversion of H$_2$cyt into Zncyt depends on the concentration of GuHCl. As the concentration of GuHCl increases, the conversion of H$_2$cyt into Zncyt increases. At

low concentrations (0.5 M GuHCl), Zncyt formation is clearly evident, however, at the end of the incorporation experiment (190 minutes), some H_2cyt remains (**Figure 5**). At low concentrations of GuHCl, H_2cyt is partially unfolded; leading to a heterogeneous mixture of folded and partially unfolded forms, each with different porphyrin exposure or accessibility to solvent.

The incorporation rate of a Zn^{2+} ion into H_2cyt was also found to be dependent on the concentration of GuHCl. At lower concentrations of GuHCl, slow incorporation of Zn^{2+} ion was observed (**Figure 5**). Under these conditions, H_2cyt is only partially unfolded with porphyrin only partially exposed to solvent taking time for the complete unfolding and the complete incorporation of the Zn^{2+} ion. At higher concentrations of GuHCl, complete and faster incorporation of Zn^{2+} ion is observed (**Figure 7**). Under these conditions, H_2cyt is completely unfolded with the porphyrin completely exposed to solvent.

The absorbance spectra obtained at lower GuHCl concentrations (0.5 M) clearly show slower incorporation with the gradual shift of the peaks from 404 nm to 423 nm over time (**Figure 5**). It also indicates that it took about 190 minutes for the complete incorporation with intermediate peaks showing the mixture of H_2cyt and Zncyt. The absorbance spectra at intermediate concentrations (2.5 M) indicate that the incorporation was fast, within few minutes (15 minutes) the Soret absorbance band shifted from 404 nm to 423 nm (**Figure 6**). The absorbance spectra at higher concentrations (4.0 M) show only a single peak at 423 nm indicating the incorporation was very fast, so fast that the conversion from H_2cyt to Zncyt could not be observed in the short time from placing the cuvette in the sample chamber and starting the collection of spectra (**Figure 7**).

The rate constants for incorporation of Zn^{2+} into H_2cyt at low and high GuHCl concentrations are summarized below. The rate constant at 0.5 M GuHCl for the decay of H_2cyt was 0.010 min^{-1}. The corresponding rate constant for the formation of Zncyt was 0.014 min^{-1} (**Figure 8**). The incorporation at higher GuHCl concentrations was very rapid, so only a few points were initially obtained before complete incorporation. This made it difficult to obtain enough data for reliable determination of the rate constants (**Figures 9 and 10**). Even so, the rate constant at 4.0 M GuHCl for the decay of H_2cyt was 0.092±0.0046 min^{-1} and the rate constant for the formation of Zncyt was 0.1060±0.0024min^{-1}. At all concentrations of GuHCl, the rate constants for decay of H_2cyt and the formation of Zncyt were similar, indicating that a single process was taking place without the formation of any intermediates. **Figure 11** shows the rate constants for formation of Zncyt initially increase as concentration of GuHCl increases. However, the rate constants plateau above 2.0 M GuHCl. At 2.0 M GuHCl, H_2cyt is already completely unfolded with the porphyrin prosthetic group completely accessible to solvent. Therefore, increased GuHCl concentration will not affect the rate of incorporation of Zn^{2+} into H_2cyt.

Incorporation of Zinc into H_2cyt as a Function of Urea. In this study, H_2cyt is dissolved in a solution of urea at various concentrations and the change in the Soret absorbance is monitored over time. The goal is to determine the effect of urea concentration on the rate of incorporation of Zn^{2+}. As the concentration of urea increases, H_2cyt should unfold and allow faster incorporation of Zn^{2+} into the porphyrin. The H_2cyt and Zncyt have significantly different heme Soret absorbance spectra, facilitating the monitoring of H_2cyt decay and Zncyt formation over time. Similar to

GuHCl, urea also effectively unfolds proteins by perturbing protein:protein, protein:solvent, and solvent:solvent interactions, such as hydrogen bonds. It differs from GuHCl in its ability to interact both on the surface and interior of the protein, facilitating the exposure of amino acid residues in the protein's hydrophobic core to water and unfolding the protein. Also being uncharged it does not show any electrostatic interactions. In our incorporation experiments, we clearly see the formation of Zncyt, indicated by the appearance of a peak at 423 nm (**Figures 12 – 14**). Moreover, the decrease in absorbance at 506 nm indicates complete incorporation of Zn^{2+} into H_2cyt (i.e., all H_2cyt has been converted into Zncyt). These observed absorbance spectra match those in the literature for Zncyt.[5]

The conversion of H_2cyt in to Zncyt depends on the concentration of urea. As the concentration of urea increases, the conversion of H_2cyt into Zncyt increases. At low concentrations (1.0 M urea), Zncyt formation is clearly evident. At the end of the incorporation experiment (285 minutes), all of the H_2cyt is converted into Zncyt (**Figure 12**). At intermediate concentrations (5.0 M urea), the incorporation was also complete (**Figure 13**). However, at high concentrations of urea (7.0 M), at the end of the incorporation experiment (57 minutes), some H_2cyt remains (**Figure 14**). This is surprising because Zn^{2+} incorporation was rapid and complete in the presence of 4.0 M GuHCl. High concentrations of urea seem to have an inhibitory affect on Zn^{2+} incorporation into H_2cyt.

The incorporation rate of a Zn^{2+} ion in H_2cyt was also found to be dependent on the concentration of urea. At lower concentrations of urea, slow incorporation of Zn^{2+} ion was observed (**Figure 12**). Under these conditions, H_2cyt is only partially unfolded

with porphyrin only partially exposed to solvent taking time for the complete unfolding and the complete incorporation of the Zn^{2+} ion. At intermediate concentrations of urea, complete and faster incorporation of a Zn^{2+}ion is observed (**Figure 13**). Under these conditions, H_2cyt is completely unfolded with the porphyrin completely exposed to solvent. However at higher concentrations (7.0 M) of urea the incorporation was not complete at the end of the experiment (57 minutes) (**Figure 14**). Maybe the time period chosen for the experiment (57 minutes) was too short to allow for complete incorporation. Comparing the incorporation of Zn^{2+} into H_2cyt at intermediate concentrations (5.0 M) and at higher concentrations (7.0 M) of urea we can conclude that at intermediate concentrations (20 minutes and complete incorporation) incorporation was faster than at higher concentrations (57 minutes and only partial incorporation). At higher concentrations (7M) the decrease in the rates may be due to protein denautration or maybe competition of urea for Zn^{+2} ion incorporation into the porphyrin ring. This clearly indicates that intermediate concentrations of urea (5.0 M) are optimal for the incorporation of Zn^{2+} in to H_2cyt.

The rate constants for incorporation of Zn^{2+} into H_2cyt at low and high urea concentrations are summarized below. The rate constant for the formation of Zncyt at the intermediate (5.0 M) concentration of urea ($k_f = 0.077\pm0.011$ min^{-1}) was two times faster than the rate constant at low (1.0 M) concentrations of urea ($k_f = 0.03200\pm0.00090$ min^{-1}) and was 1.5 times faster than at high (7.0 M) concentrations of urea ($k_f = 0.05100\pm0.00048$ min^{-1}). It can be concluded from this section that intermediate concentrations of urea (5.0 M) are optimal for the incorporation of Zn^{2+} into H_2cyt.

Incorporation of Copper into H₂cyt as a Function of Temperature.

Incorporation of Cu^{2+} facilitated by thermal unfolding of H₂cyt was analyzed using absorbance spectroscopy at increasing temperatures (40°C, 45°C, 50°C and 55°C). The goal is to determine the effect of temperature on the rate of incorporation of Cu^{2+}. The H₂cyt and Cucyt have significantly different heme Soret absorbances which help in the monitoring of the conversion of H₂cyt to Cucyt. In this study, H₂cyt is dissolved in unbuffered milliQ water and maintained at different temperatures. Then change in the Soret absorbance is monitored over time. H₂cyt is a compact structure that is susceptible to temperature-induced unfolding. Temperature as a denaturant causes unfolding by increasing the kinetic energy of the protein disrupting hydrogen bonds within the protein structure. At higher temperatures, H₂cyt unfolds and facilitates the incorporation of Cu^{2+} into porphyrin forming Cucyt.

Changes in the Soret absorbance as a function of temperature clearly indicate the complete incorporation of Cu^{2+} into H₂cyt and formation of Cucyt (**Figures 18 – 21**). The shift in Soret absorbance band from 404 nm (characteristic of H₂cyt) to 422 nm (characteristic of Cucyt) and also the change in the region of 500 to 650 nm from four absorbance maxima to two, specifically the decrease in absorbance at 506 nm is indicative of complete incorporation of Cu^{2+} into H₂cyt. These observed absorbance spectra match those in the literature for Cucyt that show that Cucyt has a single Soret absorbance band at 422 nm. This form of Cucyt is monomeric and pentacoordinate since one of the axial ligands is completely lost.[21]

The incorporation rate of Cu^{2+} in H₂cyt was also found to be dependent on the temperature. Absorbance spectra at 40°C clearly indicates slow incorporation of Cu^{2+}

with a gradual shift in the Soret absorbance band from 404 nm to 422 nm over 60 minutes (**Figure 18**). Under these conditions, H_2cyt is only partially unfolded with the porphyrin only partially exposed which increases the time for incorporation. At intermediate temperatures (45°C and 50°C) the shift in the Soret absorbance band from 404 nm to 422 nm was nearly immediate (**Figures 19 and 20**). Some H_2cyt was still observed in the first few absorbance spectra obtained after addition of Cu^{2+} to the cuvette. The absorbance spectra at higher temperatures (55°C) indicate that complete incorporation of Cu^{2+} occurs very rapidly, so that the conversion from H_2cyt into Cucyt could not be observed in the short time prior to placing the cuvette in the sample chamber and starting the collection of absorbance spectra (**Figure 21**). At intermediate and high temperatures, rapid incorporation and formation of Cucyt is a result of complete unfolding of H_2cyt and accessibility of the porphyrin to solvent.

Unfortunately, due to the rapid incorporation of Cu^{2+} into H_2cyt, rate constants could only be obtained at 40°C. Even so, the rate constants for the disappearance of H_2cyt and the formation of Cucyt were similar, indicating that a single process was taking place without the formation of any intermediates.

Incorporation of Copper into H_2cyt as a Function of GuHCl. In this study, H_2cyt is dissolved in a solution of GuHCl at various concentrations and the change in the Soret absorbance is monitored over time. The goal is to determine the effect of GuHCl concentration on the rate of incorporation of Cu^{2+}. As the concentration of GuHCl increases, H_2cyt should unfold and allow faster incorporation of Cu^{2+} into the porphyrin. The H_2cyt and Cucyt have significantly different heme Soret absorbance spectra, facilitating the monitoring of H_2cyt decay and Cucyt formation over time. Absorbance

spectroscopy can also be used to very precisely study the different conformational forms of Cucyt present at various GuHCl concentrations. The results clearly show the formation of different conformational forms Cucyt that can be resolved spectroscopically (**Figure 25**). The complete incorporation of Cu^{2+} into H_2cyt forming Cucyt is shown by the shift in Soret absorbance band from 404 nm (characteristic of H_2cyt) to 390nm, 403nm and 422 nm (characteristic of different forms of Cucyt) and also the change in the region of 500 to 650 nm from four absorbance maxima to two (**Figures 22 – 24**). Specifically the decrease in absorbance at 506 nm is indicative of complete incorporation of Cu^{2+} into H_2cyt. In all of our Cu^{2+} incorporation experiments, it appears that incorporation occurs so rapidly, by the time the cuvette is placed in the sample holder and the first spectrum collected, no H_2cyt remains. This precludes the measurement of rate constants for the incorporation of Cu^{2+} into H2cyt.

It was reported in previous studies that formation of Cucyt results in two spectroscopic forms with peaks at 403 nm and 422 nm.[21] These two spectroscopic forms show pH-dependent conformational forms. At neutral pH, the Soret absorbance band is observed at 422 nm and at extreme pH values (pH 2 or 13), the Soret absorbance band shifts to 390 nm. These different conformational forms are suggested to be due to changes in quaternary structure and copper ligand environment. The conformational form of Cucyt with peak at 422 nm is monomeric and pentacoordinate. The conformational form of Cucyt with peak at 390 nm is dimeric and tetracoordinate (no protein-donated axial ligands).

Our absorbance spectroscopy results also support the idea that different conformational forms of Cucyt exist and that they depend on the concentration of GuHCl.

At lower GuHCl concentrations (0.5 M and 1.0 M), we observed the formation of two spectroscopic forms of Cucyt with Soret absorbance bands at 403 nm and 422 nm (**Figures 22 – 23**). At 0.5 M GuHCl, there was a peak at 422 nm and a small shoulder at 403 nm. At 1.0 M GuHCl, there was a peak at 403 nm with a shoulder at 422 nm. This suggests that as GuHCl concentration increases, another conformational form of Cucyt is favored, one that is characterized by a Soret absorbance band at 403 nm. At intermediate GuHCl concentrations (1.5 M), a mixture of two conformational forms were observed, one with a Soret absorbance peak at 390 nm and another at 403 nm. At higher GuHCl concentrations (2.5 – 4.0 M), we only observed one conformation with a Soret absorbance band that is significantly blue-shifted to 390 nm (**Figure 24**). In summary, it appears that upon incorporation of Cu^{2+} into H_2cyt, at least three conformations of Cucyt simultaneously exist. The appearance and presumably the interconversion of these different conformational forms depends on the concentration of GuHCl.

Equilibrium Unfolding of Cucyt Monitored by Tryptophan Fluorescence.
Structural stability of iron cytochrome c, H_2cyt and Zncyt as a function of temperature and denaturant concentration has been well studied. However, partially and completely unfolded forms of Cucyt have not been studied before. We attempted to monitor the unfolding of Cucyt using tryptophan fluorescence. Since Cucyt contains a single tryptophan at residue 59, all the fluorescence emission intensity upon excitation at 280 nm can be attributed to that residue. Unfolding of Cucyt by denaturants like urea or GuHCl or temperature induces large changes in the tryptophan fluorescence emission intensity owing to an increase in the exposure of the tryptophan to solvent. The tryptophan fluorescence of cytochrome c is of particular interest because of the close

proximity of the single tryptophan residue at position 59 to the heme moiety.[12] The fluorescence intensity of tryptophan depends on the solvent and environmental factors, which is used as a probe to the solvent accessibility of the protein. Changes in protein conformation, such as unfolding, lead to large changes in the fluorescence emission intensity.[49] Tryptophan fluorescence emission exhibits changes in intensity and wavelength.[49] In the unfolded state of a protein, the emission maximum of tryptophan usually shifts from smaller wavelengths to 350 nm which is the emission maximum of only tryptophan without any protein residues.[49] Unfolding of Cucyt facilitates complete exposure of the tryptophan residue, and our results show a shift in the fluorescence emission to 350 nm. In the folded state when tryptophan is buried in the interior of the hydrophobic core and least accessible to solvent, fluorescence emission shifts to lower wavelengths.[49] Small changes in protein conformation result in large changes in the tryptophan fluorescence emission. Our results showing the shift in the tryptophan emission to 350 nm clearly indicates the unfolding of Cucyt as denaturant concentration increases (**Figure 26**). Cytochrome *c* unfolding also causes a decrease in the tryptophan fluorescence intensity.[49] Our results clearly show a decrease in emission intensity as concentration increases from 0.25 M to 4.0 M GuHCl (**Figure 26**).

It was reported previously that fluorescence intensity decreases with increasing temperature.[49] Our thermal-unfolding results indicate this as well. Emission spectra of lowest and highest temperature clearly show the decrease in intensity (**Figure 31**). This is also due to differences in exposure of the tryptophan residue to solvent.

Based on the tryptophan fluorescence emission results, the midpoint for the unfolding transition (C_m) and free energy of unfolding (ΔG_U) were obtained for Cucyt

under various denaturating conditions (**Figures 27 – 30**). The midpoint for the fraction unfolded curve for Cucyt in presence of GuHCl is 2.61±0.24 M and in presence of urea is it was 4.74±0.1 M. Although each denaturant unfolded proteins differently, it is evident that GuHCl is a more powerful denaturant compared to urea (less GuHCl is required to completely unfold Cucyt). Based on these observations, we can assume that at least 3.0 M GuHCl and 5.0 M urea solutions unfold Cucyt.

The ΔG_U value for Cucyt was obtained by extrapolating the free energy to zero concentration of the denaturant. The thermodynamic parameters obtained for Cucyt unfolding induced by urea compare well to the values of other cytochromes like Zncyt, iron cytochrome c and H$_2$cyt for urea induced unfolding obtained from literature.[5] The stability of unfolded Cucyt (ΔG_U = 23.8±2.3 kJ/mol) is less than iron cytochrome c (ΔG_U = 37.5 kJ/mol) and Zncyt (ΔG_U = 47.2 kJ/mol). Substitution of iron by copper decreases the structural stability of cytochrome c and is most likely due to changes in the axial ligand environment, especially since copper tends to be pentacoordinate and iron tends to be hexacoordinate in cytochrome c.

CHAPTER 5.

CONCLUSIONS

In our studies, metal substituted cytochromes (Cucyt and Zncyt) were successfully prepared. The study of the incorporation of metal ions into H_2cyt is facilitated by characteristic differences in their Soret absorbance spectra. The contamination studies as function of unfolding of H_2cyt and incorporation of metal ion in GuHCl has provided important information regarding the unfolding of proteins by GuHCl. The concentrations of GuHCl that can induce conformational changes in H_2cyt have been determined. It was shown that at low concentrations of GuHCl (0.001 M, 0.01 M and 0.1 M) conformational changes were evident, enough so to allow incorporation of contaminating metal ions. Very low concentrations of GuHCl (0.0001 M) did not induce conformational changes or alter the protein's overall tertiary structure leaving the hydrophobic core intact and the porphyrin prosthetic group buried within the protein's interior.

Chemical denaturants like GuHCl and urea, as well as increased temperature are chosen to induce H_2cyt unfolding and facilitate metal-ion incorporation. The preparation of Zncyt by unfolding H_2cyt by GuHCl was confirmed by the appearance of a Soret absorbance maximum at 423 nm. At lower concentrations of denaturants there was only partial exposure of the porphyrin prosthetic group to solvent so only slow, partial incorporation occurs. At higher concentrations of denaturants, there was complete and very rapid incorporation, owing to significant protein unfolding and exposure of the porphyrin prosthetic group to solvent. The rate constants for the disappearance of H_2cyt

and appearance of Zncyt were similar indicating that it is a single process with no intermediates. The increase in the rate constants with increase in the concentration of denaturant indicates the dominant role of denaturant concentration in the incorporation reactions.

Cucyt formation at different temperatures resulted in just one conformation with a Soret absorbance maxima peak at 422 nm, unlike that observed for Cucyt formation in the presence of GuHCl. Significant changes in the Cucyt Soret absorbance was observed at different GuHCl concentrations. These changes are suggested to be in part caused by pH changes in the GuHCl solutions that alter the axial ligation of the metal ion to the protein. At lower concentrations of GuHCl there were two Soret absorbance peaks at 403 nm and 422 nm indicating the formation of two conformational forms. At intermediate concentrations the peaks are blue shifted forming a mixture of Cucyt conformations with peaks at 390 nm and 403 nm. At higher concentrations the Soret absorbance peaks are even more blue shifted to 390 nm.

Equilibrium unfolding of Cucyt using tryptophan fluorescence emission provided information regarding the structural stability of Cucyt. Ours is the first study of this kind on Cucyt. Cucyt is less structurally stable compared to iron cytochrome c and Zncyt, but that Cucyt is significantly more structurally stable than H_2cyt. Little research has been done in separating the Cucyt conformational forms (that were resolved spectroscopically) and investigating their structural and functional properties. This opens up a new direction for future research on Cucyt and other metal-substituted cytochromes.

REFERENCES

1. Garrett, R.H.; Grisham, C.M. *Biochemistry* 2nd Edition, Thomson Brooks/Cole, Pacific Groove, CA, **1999**.

2. Lippard, S.J.; Berg, J.M. *Principles of Inorganic Chemistry*, University Science Books, Mill Valley, CA, **1994**.

3. Turano, P. *Inorg. Chem.* **2004**, *43*, 7945-7952.

4. Tanaka, M. *Pure & Appl. Chem.* **1983**, *55*, 151-158.

5. Tremain, S.M.; Kostic, N.M. *Inorg. Chem.* **2002**, *41*, 3291-3301.

6. Scott, R.A.; Mauk, A.G. *Cytochrome c: A multidisciplinary Approach*, University Science Books, Mil Valley, CA, **1996**.

7. Chein, J.C.W. *J. Phy. Chem. Soc.* **1978**, *82*, 2171-2179.

8. Fisher, W.R.; Taniuchi, H.; Anfinsen, C.B. *J. Bio. Chem.* **1973**, *248*, 3188-3195.

9. Slama, J.T.; Smith, H.W.; Wilson, C.G.; Rapoport, H. *J. Am. Chem. Soc.* **1975**, *97*, 6556-6562.

10. Babul, J.; Stellwagen, E. *Biochemistry* **1972**, *11*, 1195-1200.

11. Ma, J.; Laberge, M.; et.al. *Biochemistry* **1998**, *37*, 5118-5128.

12. Brems, D.N.; Liu, Y.C.; Stellwagen, E. *J. Bio. Chem.* **1982**, *257*, 3864-3868.

13. Vanderkooi, J.M.; Adar, F.; Erecinksa, M. *Eur. J. Biochem.* **1976**, *64*, 381-387.

14. Strottmann, J.M.; Stellwagen, A.; Bryant, C.; Stellwagen, E. *J. Bio. Chem.* **1984**, *259*, 6931-6936.

15. Monera, O.D.; Kay, C.M.; Hodges, R.S. *Pro. Sci.* **1994**, *3*, 1984-1991.

16. Manger, E.; McLendon, G. *J. Phys. Chem* **1989**, *93*, 7130-7134.

17. Glatz, P.; Chance, B.; Vanderkooi, J.M. *Biochemistry* **1979**, 3466 - 3470.

18. Chein, J.C.W. *J. Am. Chem. Soc.* **1978**, *100*, 1310-1312.

19. Vanderkooi, J.M.; Chance, B.; Waring, A. *FEBS Lett.* **1978**, *88*, 273-274.

20. Findlay, M.C.; Dickinson, L.C.; Chein, J.C.W. *J. Am. Chem. Soc.* **1977**, *99*, 5168-5173.

21. Shelnutt, J.A.; Straub, K.D.; Rentzepis, P.M.; Gouterman, M.; Davidson,

E.R. *Biochemistry* **1984**, *23*, 3946-3954.

22. Funahashi, S.; Inada, Y.; Inamo, M.; *Anal. Sci.* **2001**,*17,* 917-927.

23. Ghelis, C.; Yon, J. *Protein Folding*, Academic Press, London, **1992**.

24. Fleischer, E.B.; Wang, J.H. *J. Am. Chem. Soc.* **1960**, *82*, 3498-3502.

25. Bailey, S.L.; Hambright, P. *Inorg. Chem. Acta* **2003**, *344*, 43-48.

26. Hambright, P.; Chock, P.B. *J. Am. Chem. Soc.* **1974**, *96*, 3123-3131.

27. Fleischer, E.B.; Choi, E.I. *Inorg. Chem.* **1963**, *2*, 94-97.

28. Fleischer, E.B.; Choi, E.I.; Hambright, P.; Stone, A. *Inorg. Chem.* **1964**, *3*, 1284-1287.

29. Vanderkooi, J.M.; Landesberg, R.; Hayden, G.W.; Owen, C.S. *Eur. J. Biochem.* **1977**, *81*, 339-347.

30. Dickinson, L.C.; Chein, J.C.W. *Biochemistry* **1975**, *14*, 3526-3532.

31. Zhou, J.S.; Nocek, J.M.; DeVan, M.L.; Hoffman, B.M *Science* **1995**, *269*, 204-207.

32. Kim, J.E.; Pribisko, M.A.; Gray, H.B.; Winkler, J.R. *Inorg. Chem.* **2004**, *43*, 7953-7960.

33. Anni, H.; Vanderkooi, J.M.; Mayne, L. *Biochemistry* **1995**, *34*, 5744-5753.

34. Qian, C.; Yao, Y.; Tong, Y.; Wang, J.; Tang, W. *J. Biol. Inorg. Chem.* **2003**, *8*, 394-400.

35. Baker, H.; Hambright, P.; Wagner, L.; Ross, L. *Inorg. Chem.* **1973**, *12*, 2200-2202.

36. Sciffer, C.A.; Dotsch, V.; Wuthrich, K.; van Gunsteren, W.F. *Biochemistry* **1995**, *35*, 15057-15067.

37. Tabata, M.; Babasaki, M. *Inorg. Chem.* **1992**, *31*, 5268-5271.

38. Dunbar, J.; Yennawar, H.P.; Banarjee, S.; Luo, J.; Fabber, G.K. *Pro. Sci.* **1997**, *6*, 1727-1733.

39. Bennion, B.J.; Daggett, V. *Proc. Natl. Acad. Sci.* **2003**, 100, 5142-5147.

40. Russell, B.S.; Bren, K.L. *J. Biol. Inorg Chem.* **2002**, *7*, 909-916.

41. Bhuyan, A.K. *Biochemistry* **2002**, *41*, 13386-13394.

42. Russell, B.S.; Bren, K.L.; Melenkivitz, R. *PNAS* **2000**, *97*, 8312-8317.

43. Latypov, R.F.; Cheng, H.; Roder, N.A.; Zhang, J.; Roder, H. *J. Mol. Biol*

2006 1-17.

44. Akiyama, S.; Takahashi, S.; Kimura, T.; Oishimori, K.; Morishima, I.; Nishikawa, Y.; Fujisawa. T. *Proc. Natl. Acad. Sci.* **2002**, 99, 1329-1334.

45. Lee, J.C.; Chang, I-Jy.; Gray, H.B.; Winkler, J.R. *J. Mol. Biol.* **2002**, *320,* 159-164.

46. Lesch, H.; Stadlbauer, H.; Fredrich, J.; Vanderkooi, J.M.; *Biophys. J.* **2002**, *82,* 1644-1653.

47. Wilson, A.J.; Groves, K.; Jain, R.K.; Park, H.S.; Hamilton, A.D. *J. Am. Chem. Soc.* **2003**, *125*, 4420-4421.

48. Logovinsky, V.; Vanderkooi, J.M.; Kaposi, A.D. *Biochim. Biophys. Acta* **1993**, *1161*, 149-160.

49. Creighton, T.E. *Protein Structure: A Practical Approach*, Oxford University Press, New York, **1997.**

50. Debnath, B.S.; Haque, E.; Ray, S.; Chakrabarti, A. *Indian Journal of Biochem. & Biophys.* **2001**, *38,* 84-89.